The Geological Society

Earth Science, Systems and Society

ORIGINAL RESEARCH
published: 21 November 2022
doi: 10.3389/esss.2022.10056

Heat Recovery Potential and Hydrochemistry of Mine Water Discharges From Scotland's Coalfields

David B. Walls[1], David Banks[2], Tatyana Peshkur[1], Adrian J. Boyce[3] and Neil M. Burnside[1]*

[1]Department of Civil and Environmental Engineering, University of Strathclyde, Glasgow, United Kingdom, [2]James Watt School of Engineering, University of Glasgow, Glasgow, United Kingdom, [3]Scottish Universities Environmental Research Centre, East Kilbride, United Kingdom

Prospective and operational mine water geothermal projects worldwide have faced challenges created by mine water chemistry (e.g., iron scaling, corrosion) and high expenditure costs (e.g., drilling or pumping costs) among others. Gravity fed or actively pumped drainages can be cheaper sources of low-carbon mine water heating when coupled with adequately sized heat exchanger and heat pump hardware. They also provide valuable chemical data to indicate mine water quality of associated coalfields. Field collection of temperature and flow rate data from mine water discharges across the Midland Valley of Scotland, combined with existing data for Coal Authority treatment schemes suggest that mine water heat pumps could provide a total of up to 48 MW of heat energy. Chemical characterisation of mine waters across the research area has created a valuable hydrochemical database for project stakeholders investigating mine water geothermal systems using boreholes or mine water discharges for heating or cooling purposes. Hydrochemical analytical assessment of untreated gravity discharges found that most are circumneutral, non-saline waters with an interquartile range for total iron of 2.0–11.6 mg/L. Stable isotope analysis indicates that the discharges are dominated by recent meteoric waters, but the origin of sulphate in mine waters is not as simple as coal pyrite oxidation, rather a more complex, mixed origin. Untreated gravity discharges contribute 595 kg/day of iron to Scottish watercourses; thus, it is recommended that when treatment schemes for mine water discharges are constructed, they are co-designed with mine water geothermal heat networks.

Keywords: isotopes, geochemistry, mine water, low-carbon, thermal resource, geothermal, iron, renewable heating

OPEN ACCESS

Edited by:
Jack Longman,
University of Oldenburg, Germany

Reviewed by:
Mohammad Arzoo Ansari,
Bhabha Atomic Research Centre (BARC), India
Gareth Farr,
Coal Authority, United Kingdom
Ting Bao,
Michigan Technological University, United States
Andrew Fraser-Harris,
University of Edinburgh, United Kingdom

***Correspondence:**
Neil M. Burnside
neil.burnside@strath.ac.uk

Received: 26 April 2022
Accepted: 28 October 2022
Published: 21 November 2022

Citation:
Walls DB, Banks D, Peshkur T, Boyce AJ and Burnside NM (2022) Heat Recovery Potential and Hydrochemistry of Mine Water Discharges From Scotland's Coalfields. *Earth Sci. Syst. Soc.* 2:10056. doi: 10.3389/esss.2022.10056

INTRODUCTION

Decarbonisation of heating and cooling is essential if we are to decrease anthropogenic emissions and combat climate change. For example, heat production accounts for 45% of energy use and 32% of CO_2 emissions in the UK (Crooks, 2018). Mirroring global efforts (United Nations, 2019), the UK government has committed to reaching net zero greenhouse gas emissions by 2050 (UK Government, 2021a; UK Government, 2021b) and has mandated the end of fossil-fuel heating systems in all new build homes by 2025 (Committee on Climate Change, 2019). The Scottish Government has committed to net zero emissions by 2045 (Scottish Government, 2020) and is proposing to ban fossil-fuel heating systems in new buildings by 2024

(Scottish Government, 2022). Decarbonisation of heating and cooling has challenges different to that of other energy requirements (e.g., electrical power) since the former requires decentralised generation and consumption. Heating still has an overreliance on fossil fuels and is dependent on seasonal weather conditions. In 2020, only 6.4% of Scotland's overall non-electrical heat supply was from renewable technologies, far from the 2020 target of 11% (Energy Saving Trust, 2021).

The heating and cooling resource represented by abandoned, flooded mine workings has been portrayed as having significant thermal energy potential (Adams et al., 2019). Flooded coal mines contain vast volumes of mine water in close proximity to housing and industry stock at between 10˚C and 36˚C (Farr et al., 2021) which can be exploited to provide a thermal load *via* low-carbon heating and cooling networks (Verhoeven et al., 2014). The Midland Valley of Scotland (MVS) alone has estimated mine water geothermal reserves of 12 GW, which given favourable conditions (accessibility and building stock quality) could provide over one third of Scotland's annual domestic heat demand (33 GW) (Gillespie et al., 2013). There is no doubt that if these resources could be utilised in a cost-effective manner, they would be a major benefit in efforts to displace fossil fuels from heat production — turning former environmental liabilities into potentially valuable low-carbon assets.

Historically, removal of mineral material from underground coal mines in Scotland created void spaces at depths ranging from outcrop at surface to a little over 1,000 m below ground level (BGL), with varying degrees of connectivity. As well as creating underground flooded void space ("anthropogenic karst" (Younger and Adams, 1999)) mining also enhances the porosity and permeability of adjacent aquitard and aquifer units by collapse and fracturing (Ó Dochartaigh et al., 2015). Most of the abandoned mines in the MVS are former coal mines, but others include ironstone, limestone, oil-shale, and various metals (gold, silver, lead etc.) (Gillespie et al., 2013).

The use of open loop abstraction-reinjection (well doublet) heat exchange systems based on shallow groundwater is globally widespread (Jessop et al., 1995; Verhoeven et al., 2014; Ramos et al., 2015; Walls et al., 2021; Monaghan et al., 2022a; Banks et al., 2022), and is similar to configurations found in other geothermal reservoir types such as hot dry rock and hot sedimentary aquifers (Limberger et al., 2018; Reinecker et al., 2021). However, there are alternative configurations by which mine water's thermal energy can be harnessed (Banks et al., 2019; Walls et al., 2021), each accompanied by varying drilling costs and project risks (Monaghan et al., 2022b). Detailed understanding of mine water geothermal energy resource size and sustainability remains largely in its research phase, with increasing numbers of projects being started (Walls et al., 2021; Monaghan et al., 2022a; Banks et al., 2022). Owing to the heterogeneous nature of mine workings, each project has unique hydrogeological properties, thus uncertainty around the speed and extent of heat migration within mines and initial resource scale and availability are regarded as significant project risks during the planning stage (Walls et al., 2021). Existing pumped or gravity mine water discharges, which do not require exploratory drilling or pumping tests, are therefore appealing for development (Bailey et al., 2016). Gravity discharges may emerge at the surface *via* mine adits or shafts (Younger and Adams, 1999), or "break out" at the lowest hydrological point, e.g., a river, even when there is no shaft or adit present. Their temperature, flow and estimated heat resource have either been recorded for ongoing environmental monitoring purposes or can easily be measured onsite (Wood et al., 1999). In certain circumstances, mining authorities (such as The Coal Authority (TCA) in Great Britain) deliberately pump boreholes or shafts, where it is deemed necessary to prevent uncontrolled surface outbreak (Bailey et al., 2016) or contamination of important water aquifers (Bailey et al., 2013) above mine water systems. Further afield, other countries have similar pumping arrangements to protect adjacent mine workings (Janson et al., 2016). The high loading of iron in many of the larger gravity and pumped discharges means that mine water treatment is required, often by passive aeration-precipitation-settlement-retention systems, involving lagoons and wetlands (Banks and Banks, 2001; Banks, 2003). Whilst this paper mainly focusses on gravity drainages from mines across Scotland, it includes the details of TCA pumping and treatment sites to improve the accuracy of potential heating estimates for mine water resources present at surface.

Water levels in UK coal mines were artificially lowered by dewatering throughout the 18th–20th centuries (Younger and Adams, 1999). Initially, water "levels" or adits were used to drain mines by gravity to river valleys. As mining progressed deeper, pumping stations and engine houses were employed to keep the water table depressed at a safe level for mining activities, and manage water levels across interconnected coalfields (Wallis, 2017). The cessation of pumping following closure of collieries allowed groundwater to rebound to pre-mining levels. Interconnected mine voids remain the preferential flow pathway for groundwater where the water table has fully recovered following cessation of pumping, and these continue to drain mine water to the surface *via* shafts, drifts and adits (Younger and Adams, 1999). The network of coal mines which these pathways drain can be regional, with connections to numerous collieries, e.g., Fordell day level in Fife (Rowley, 2013). Younger and Robins (2002) predicted that the unmitigated impacts of mine water recovery and break out could include: risks of contamination of surface water bodies by high concentrations of iron, manganese or sulphate (Younger, 2000a); flooding of agricultural, industrial or residential areas (Younger and LaPierre, 2000); and contamination of important aquifers overlying coal seams (Bailey et al., 2013). Other impacts include an increased subsidence risk as the rising waters weaken previously dry, shallow workings (Smith and

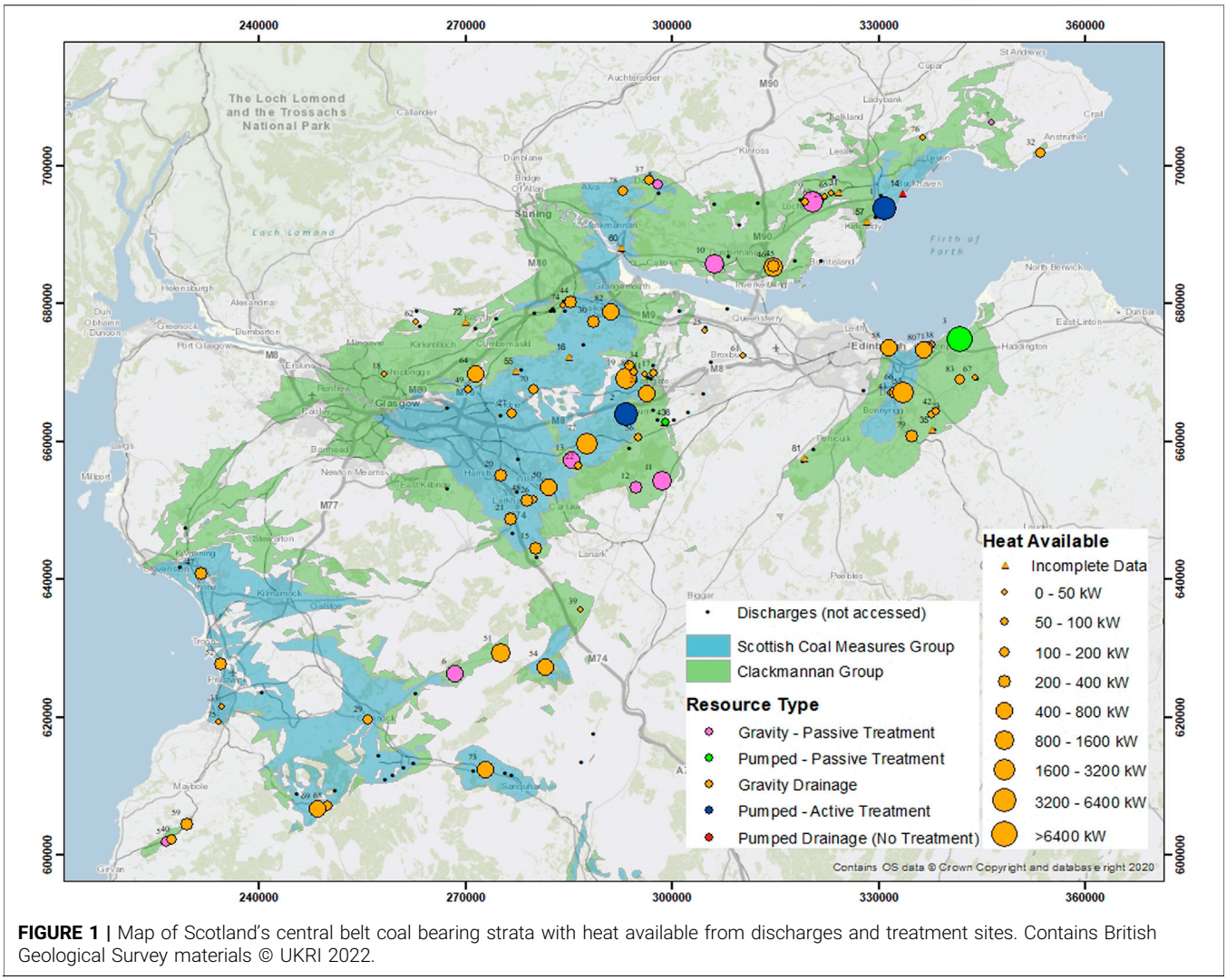

FIGURE 1 | Map of Scotland's central belt coal bearing strata with heat available from discharges and treatment sites. Contains British Geological Survey materials © UKRI 2022.

Colls, 1996), or transportation of mine gases to the surface, displaced from pore spaces by the rising waters (Hall et al., 2005). The annual flow of some discharges may fluctuate (Environmental Agency, 2021), especially if associated with shallow workings or sink holes, responding immediately to rainfall and recharge events (Farr et al., 2016). For example, the Jackson Bridge mine water discharge, in Holmfirth, Yorkshire, normally visually affects the local river with ferric iron for 5 km downstream, but after heavy rainfall the river turned orange for 60 km (Environmental Agency, 2021). Interception of these rising waters, before or following surface break out, is an opportunity to prevent impacts and engineer a local, renewable heating source.

Gravity drainages can provide a source of low-carbon heating or cooling when coupled to appropriate thermal infrastructure in the form of heat exchangers and heat pumps. Since subsurface engineering is not required, gravity drainages represent a real opportunity for low-cost, low-risk resource utilisation when compared to schemes which require drilling of boreholes into multiple seams. For discharges which respond to seasonal rainfall, increased mine water fluxes fortunately correlate with periods of increased heating demand across colder months of the year (Farr et al., 2016). Other discharges, which are often deeper sourced, show consistent flowrates independent of rainfall anomalies (Mayes et al., 2021) which makes heat delivery consistent and reliable. This study presents heating potential and water chemistries, and therefore, the scale of an easily accessible low-carbon heating and cooling resource within the MVS. If sensibly harnessed, mine water gravity discharges can play a role in the decarbonisation of Scotland's heating infrastructure.

Geological Setting

This study focusses on the principal mining regions of Scotland, covering the Central, Lothians, Fife, Ayrshire and Douglas coalfields. The associated coal bearing strata of the Carboniferous in the Midland Valley of Scotland terrane extend for approximately 150 km in an ENE trending block, 50 km wide, from Ardrossan and

TABLE 1 | Sedimentary successions from the Carboniferous for the West Lothian area of the Midland Valley of Scotland. Other areas host variations within the Strathclyde Group. Modified from (Monaghan, 2014) and (Waters et al., 2007).

Age	Group	Formation	Dominant Lithologies	Economic mineral
Westphalian	Scottish Coal Measures Group	Scottish Upper Coal Measures Formation	Sandstone, siltstone, mudstone, minor coal	Minor Coal
		Scottish Middle Coal Measures Formation	Sandstone, siltstone, mudstone, coal	Coal
		Scottish Lower Coal Measures Formation	Sandstone, siltstone, mudstone, coal	Coal
Namurian	Clackmannan Group	Passage Formation	Sandstone, conglomerate and mudstone	
		Upper Limestone Formation	Limestone, mudstone, siltstone, sandstone, coal	Coal
Visean		Limestone Coal Formation	Sandstone, siltstone, mudstone, coal	Coal
		Lower Limestone Formation	Limestone, mudstone, siltstone, sandstone	
	Strathclyde Group	West Lothian Oil Shale Formation	Oil-shale, sandstone, siltsone, mudstone	Oil-Shale
		Gullane Formation	Sandstone, mudstone, siltstone	
Tournasian	Inverclyde Group	Clyde Sandstone Formation	Sandstone	
		Ballaghan Formation	Siltstone, dolostone, minor evaporites	
		Kinnesswood Formation	Sandstone	

Girvan in the west to St Andrews and Haddington on the east coast (Cameron and Stephenson, 1985) (**Figure 1**). The MVS terrane is a graben structure bounded by the Highland Boundary Fault to the north and the Southern Upland Fault to the south (Bluck, 1984). As a sedimentary basin, it opened in the Lower Palaeozoic and preserves Silurian to Permian age sedimentary rocks (Cameron and Stephenson, 1985). The Carboniferous sedimentary successions and their relevant economic minerals are described in **Table 1**. Igneous activity across the area contributed to volcanic centres which now stand as elevated areas, e.g. the Kilpatrick, Campsie and Ochil hills; and subsurface activity cut the sedimentary sequences with a series of dykes and sills (Trueman, 1954). Depositional accommodation space, created as part of the transtensional strike-slip fault regime (Underhill et al., 2008), generated several smaller basins which show syntectonic deformation thickness variations (Rippon et al., 1996). Whilst coal seams across Scotland are found primarily in the Carboniferous successions within the MVS, the units extend into the Southern Upland Terrane, with further outliers hosted near Campbeltown in Kintyre, and in the Jurassic sedimentary successions of the Moray Firth at Brora (Trueman, 1954).

Early records of coal mining in Scotland date back to the 12th century, whereby monasteries were granted rights to extract coal, but the intensity of coaling increased significantly with the beginnings of the industrial revolution (Younger and Robins, 2002). Scottish coal was extensively mined in the Namurian Limestone Coal Formation of the Clackmannan Group and the stratigraphically higher Lower and Middle Scottish Coal Measures Formations of the Westphalian. Both the Limestone Coal and the Scottish Coal Measures host many workable coal seams amongst a cyclical stratigraphy of sandstones, siltstones, mudstones and shales (Cameron and Stephenson, 1985). Despite its name, the Limestone Coal Formation does not contain abundant limestone strata. The oil shales that are mined in some regions (e.g., West Lothian) are also held in Carboniferous strata (e.g., Visean), stratigraphically adjacent or subjacent to the coal bearing formations (Monaghan, 2014).

Hydrogeological Setting

The hydrogeological properties of unmined Carboniferous coal bearing units in Scotland differ significantly to those of mined regions (Ó Dochartaigh et al., 2015). The sandstone horizons of the sequences host the greatest permeabilities but tend to be fine grained, well cemented and interbedded with lower permeability mudstones, siltstones and coals (Ó Dochartaigh et al., 2015). Groundwater movement in unmined regions is dominated by fracture flow, where host rock matrix permeabilities are in the range of 0.0003–0.1 m/d, and operational yields of 1.5–4.8 L/s are recorded by Ó Dochartaigh et al. (2015). Conversely, mined seams represent anthropogenic aquifers which have greatly increased aquifer transmissivity and can link formerly separate aquifer units laterally and vertically. The range of operational yields from boreholes and wells completed into mined strata in Scotland is large, from 0.5 L/s to 257.5 L/s (Ó Dochartaigh et al., 2015), with flow regimes in the mined aquifers often being non-laminar (Younger and Adams, 1999). The common occurrence of a 1–2 m thick zone of significantly fractured or deformed rock mass above and below workings may have implications for overall hydraulic conductivity and storativity by creating preferential flow pathways and inducing adjacent porous media flow (Monaghan et al., 2022b). As an example of the extent of mine working connectivity, the South Lanarkshire Farme Colliery, when active, was connected to other collieries over a scale of kilometres (Monaghan et al., 2017; Monaghan et al., 2022b). However the groundwater flow properties in mine workings (Younger and Adams, 1999) and their response to pumping (Banks, 2021; Banks et al., 2022) remain largely unpredictable before system installation and hydraulic characterisation. Similarly, temporal evolution of groundwater hydraulics in shallow mines may have implications for mine water thermal abstraction (Andrews et al., 2020).

Mine Water Chemistry

The processes which influence coal mine water chemistry are well documented (Banks et al., 1997; Younger, 2000b; Burnside et al., 2016a; Banks et al., 2019). Mine water discharges can be alkaline, acidic, ferruginous, saline, reducing, oxidising or relatively uncontaminated. Subsequent impacts of mine water chemistry on geothermal system infrastructure can include clogging and corrosion among others (Steven, 2021; Walls et al., 2021). Sulphide minerals which are present in coal-bearing strata or other mineral seams/veins, are susceptible to oxidation when exposed to air. Pyrite, in particular, is commonplace in coal bearing strata and when oxidised, reacts to release sulphate and soluble iron salts. The net processes are shown in **Eq. 1** (Banks et al., 1997).

$$2FeS_2 + 2H_2O + 7O_2 = 2Fe^{2+} + 4SO_4^{2-} + 4H^+_{(aq)}$$

$$Pyrite + water + oxygen = ferrous\ iron + sulphate + acid \quad (1)$$

Mine drainage in Scotland typically comprises mineralised water with elevated concentrations of Ca, HCO_3^-, SO_4^{2-}, Fe and Mn (O Dochartaigh et al., 2011). Circum-neutral pH values and high alkalinities suggest substantial dissolution of carbonate minerals by the acid derived from **Eq. 1** (Younger, 2001). Dissolution of carbonate minerals such as calcite ($CaCO_3$), dolomite ($Ca,Mg(CO_3)_2$), siderite ($FeCO_3$) and ankerite ($Ca(Fe,Mg,Mn)(CO_3)_2$) elevate concentrations of base cations and provide an additional potential source of dissolved iron (Banks et al., 2019).

Groundwater rebound within mined voids dissolves sulphate and metal ions from rock faces and can carry resulting solutes to the surface. Extensive oxidation prior to water table rebound has historically induced "first-flush" peak iron loads around one order of magnitude greater than long-term iron concentrations (Younger, 1997; Younger, 2000b; Gzyl and Banks, 2007). Discharged water is often clear at the outflow point since reducing conditions retain iron and manganese in solution. Following oxidation at surface, metal (oxy)hydroxides are precipitated and deposited, usually as orange "ochre" (ferric oxyhydroxide) on receiving channel beds. Ochre smothering in watercourses blocks sunlight and retards photosynthesis leading to serious deterioration in biological indices of water quality (Younger, 2000a).

Study of mine water discharges provides an inexpensive means to understand and monitor mine water properties across a region. Evidence for stratification of water chemistries in mined sequences (Nuttall and Younger, 2004; Loredo et al., 2017) means that sampled gravity discharges will tend to over-represent relatively shallow portions of mine water systems, however, the discharge chemistry provides a readily accessible proxy for the conditions in the mines. Dissolved ferrous iron in coal mine waters is often assumed to be predominantly derived from pyrite oxidation, but it may alternatively result from dissolution of iron-containing carbonates (Banks et al., 1997) or conceivably even from reductive dissolution of ferric oxides or oxyhydroxides (Stumm and Sulzberger, 1992; Peiffer and Wan, 2016; Haunch and McDermott, 2021). Where dissolution of iron carbonate predominates, it can generate water chemistries with elevated iron and bicarbonate alkalinity, but relatively little sulphate (<100 mg/L) (Younger, 2000a). Oil shale mines, found primarily in West Lothian (Monaghan, 2014), and coal mines can both be influenced by dissolution of iron sulphides (pyrite) and iron carbonates (siderite, ankerite). However, siderite tends be more prominent in freshwater sedimentary sequences and pyrite in increasingly brackish or marine sedimentary sequences (Spears and Amin, 1981). It is recognised that much of the deposition of the West Lothian Oil Shales took place in fresh-brackish lacustrine environments and that siderite is an important component of the sequence (Jones, 2007; Dean et al., 2018). One can thus speculate that iron carbonate dissolution may be more prominent in Scottish oil shale mines than coal mines—if so, one would expect lower sulphate contents in oil shale mine water.

Isotopic characterisation of water as measured by $\delta^{18}O$ and δ^2H (as ‰, against those ratios in the standard V-SMOW[1]), can help decipher the age and interaction histories of the mine water (Burnside et al., 2016b). Sulphur isotopic values, $\delta^{34}S$, give insight into the source and history of mine water sulphate (Burnside et al., 2016a; Janson et al., 2016; Banks et al., 2020). Pyrite oxidation typically results in negligible S-isotopic fractionation in resulting sulphate relative to the source sulphide (Chen et al., 2020). $\delta^{34}S$ values of pyrites (n = 21) in East Ayrshire coals range between -26.3‰ and +18.4‰ with an overall mean (cleat and banded pyrite) of +2.7‰ (Bullock et al., 2018). Studies have found that the mean values for deep mine waters in Europe can be around +20‰, and occasionally heavier (Banks et al., 2020). Speculation of the controlling factors on sulphur fractionation contributing to the additional heavy sulphate has led to hypotheses including dissolution of sulphate-bearing evaporite horizons within overlying or adjacent strata (Chen et al., 2020), residual marine waters, residual evaporative brines, and bacterial or thermal sulphate reduction reactions (Banks et al., 2020). Seawater $\delta^{34}S$ values show a decreasing trend from +21‰ to +12‰ through the Carboniferous, where periods hosting the principle coal seams in Scotland (Namurian and Westphalian) show values of c. +14‰ to +16‰ (Kampschulte et al., 2001).

MATERIALS AND METHODS

Existing Data

Bailey et al. (2016) have compiled data and estimated thermal recovery potential for 12 mine water treatment schemes owned and operated by TCA in Scotland (**Table 2**). Additionally, there is a council operated treatment site near Allanton (55.7952˚N, 3.8276˚W) treating an overflow of water from Kingshill Colliery (James Hutton Institute, 2016). Data for

[1] $(R_{sample}/R_{standard})$ - 1) x 1,000 = ∂ value; where R = $^{34}S/^{32}S$, $^{18}O/^{16}O$, $^2H/^1H$—resulting in $\delta^{34}S$, $\delta^{18}O$ and δ^2H respectively.

TABLE 2 | Coal Authority treatment sites in Scotland (Bailey et al., 2016).

Coal Authority treatment scheme	Ref no.	Treatment type	Northing (°)	Easting (°)
Frances	1	Pumped – Active	56.1327	−3.1120
Polkemmet	2	Pumped – Active	55.8573	−3.7044
Blindwells	3	Pumped – Passive	55.9627	−2.9341
Cuthill	4	Pumped – Passive	55.8485	−3.6138
Dalquharran	5	Gravity – Passive	55.2799	−4.7308
Kames	6	Gravity – Passive	55.5121	−4.0843
Lathallan Mill	7	Gravity – Passive	56.2462	−2.8655
Mains of Blairingone	8	Gravity – Passive	56.1583	−3.6434
Minto	9	Gravity – Passive	56.1391	−3.2808
Pitfirrane	10	Gravity – Passive	56.0549	−3.5077
Pool Farm	11	Gravity – Passive	55.7708	−3.6169
Wilsontown (Mousewater)	12	Gravity – Passive	55.7611	−3.6769

each treatment site summarised from existing literature and data sources can be found in **Supplementary Appendix SA**.

Identifying Sample Locations

At the start of the 21st Century, Scotland had 167 known mine water discharges in the MVS, with a total of 180 km of water courses affected by ochre (Younger, 2000a). We were provided with 153 locations of mine water discharges, believed to be associated with historic mining activities, which in 2000 were freely draining following coalfield-wide groundwater recovery towards pre-mining levels (Haunch pers. comm., 2020).

Finding discharges relied upon identification of orange ochreous stream bed staining or a distinctive H_2S gas odour, indicative of potential microbial reduction of mine water sulphate. Any mine water discharges which may have been clear, colourless and without a smell or iron staining would have been overlooked, however, any streams or flowing water found near to the original grid references were sampled for at least temperature and conductivity as indicative properties. Additionally, some natural groundwater discharges can be iron- or sulphide-rich, so the diagnostic criteria could not definitively confirm investigated waters as coal mine drainage. As a result, 66 of the 153 sites previously identified were analysed for this study. Some sites were identified but deemed unsuitable for sampling due to health and safety risk, e.g., Kincardine (#60[2]) which appeared as deep ochreous water within 5 m of an active railway line; lack of clarity of where to sample a "pure" mine water source; or cessation of flow. Five significant gravity discharges have been omitted due to access or safety reasons, in these instances data on flow rates, locations and iron concentrations have been taken from (Whitworth et al., 2012) and their heating potential included in the results section, and shown in **Supplementary Appendix SA**.

Of the 66 sampled discharges, 64 are believed to be related to coal mines and 2 to oil shale mines, the latter typically associated with the Visean West Lothian Oil-Shale Formation. There are no discharges exclusively from limestone mines, but discharges related to coal seams may source water from adjacent worked limestone units, e.g., Wallyford Great (Watson, 2007). Of the 64 coal mine discharges, 26 are believed to be derived from mines or strata in the Westphalian Scottish Coal Measures Formation, while 38 are believed to be derived from mines in the Namurian Limestone Coal Formation.

Field Sampling and Onsite Analysis

Throughout September and October of 2020, each of the 153 sites were visited with the primary aim to identify the precise location of the discharges, describe their source and characteristics, take initial physicochemical, temperature, and flow rate readings. The initial scouting exercise was to inform and streamline focused sampling trips for laboratory analyses. At each site the discharge was sampled as close to the emergence and as safely possible. A handheld Myron P Ultrameter was used to determine discharge pH, temperature, oxidation reduction potential (ORP) and electrical conductivity (EC). Recorded pH and EC values were automatically corrected to a standard temperature of 25°C. ORP was measured in millivolts (mV) and read from a platinum sensor and a silver chloride (Ag/AgCl)-saturated KCl reference electrode. ORP values were 199 mV lower than true Eh from a standard hydrogen electrode (Robinson pers. comm., 2022) but are presented here without adjustment. Equipment was calibrated before each day's fieldwork and all water samples were refrigerated as soon as possible after collection.

Total alkalinity was determined as mg/L equivalent of $CaCO_3$ with a Hach Model 16,900 digital titrator, using 1.6 N sulphuric acid and bromcresol green—methyl red pH indicator. Recorded values in mg/L $CaCO_3$ equivalent were then converted to meq/L (by dividing by 50.04 mg meq^{-1}). The alkalinity is assumed to be predominantly in the form of HCO_3^- at circumneutral pH values.

[2]The reference number preceded by the # symbol, aligns with the ordering system in **Supplementary Appendices SA,B**.

Separate aliquots were taken at site for different analyses. Filtration, to remove any particulate matter, was carried out using a hand-held, syringe mounted filter capsule. An aliquot for major anion analysis was filtered at 0.45 µm into 15 ml polypropylene screw-cap vials, with 2 ml decanted into custom vials for laboratory alkalinity analysis. An aliquot for dissolved elemental content was filtered at 0.45 µm into a 15 ml polypropylene screw cap vials and preserved using one drop of concentrated HNO_3 (68%, trace metal grade, Fisher Chemicals). An unfiltered aliquot for total (dissolved and undissolved) elemental content was collected using a clean 15 ml polypropylene screw cap vial. An aliquot for $\delta^{18}O$ and $\delta^{2}H$ analysis was taken using clean 15 ml polypropylene screw-cap vials, sealed with Parafilm to prevent sample evaporation. Three meteoric control $\delta^{18}O$ and $\delta^{2}H$ aliquots were taken monthly between December 2016 and February 2020 from the rooftop of the Rankine Building, University of Glasgow (55.8728°N, 4.2857°W). A 1 L unfiltered aliquot of sample water was collected in a plastic flask for sulphate-$\delta^{34}S$ analysis. Sulphate was subsequently precipitated as barium sulphate, using the method of Carmody et al. (1998): namely, the sample was acidified to pH 3–4 by dropwise addition of concentrated HCl (37% Trace Metal Grade, Fisher Chemicals) and then dosed with excess 5% $BaCl_2$ solution. A rapid cloudy reaction indicated the presence of sulphate *via* $BaSO_4$ precipitation.

Flow rate was calculated by measuring each stream channel's dimensions. The flow rate Q (cm^3/s) is estimated from **Eq. 2**, where depth and width are in cm, and V is velocity, measured in cm/s. The correction factor of 0.5 is applied to account for the irregular flow cross section and slower flow at the channel edges.

$$Q = Depth \times Width \times V \times 0.5 \quad (2)$$

The width of the flow channel at the surface (cm) and the depth of the flow channel (cm) were measured with a ruler or tape measure. The flow speed of the channel (cm/s) was measured by dropping a buoyant item (normally leaf or grass) into the flow and measuring distance covered in 1 s. Flow rates in cm^3/s were then multiplied by 0.001, to obtain a discharge in L/s. In other instances where the flow was from a discrete source and of a low flow rate, it was measured by timing the filling of a 1 L flask.

Finally, notes and photographs were recorded to detail each individual sample point. Notes included: the presence/intensity of H_2S gas smell; the source of the drainage (identified as closely as safely possible); the colour and turbidity of the mine water; and the size and colour of flocs suspended in the water. Each of these additional data points can be found alongside images of the discharges in **Supplementary Appendix SB**.

Laboratory Hydrochemical Analytical Methods

Of the 66 discharge samples identified, 57 were sampled for chemical analysis. All hydrochemical analyses were completed in the laboratories of the Department of Civil and Environmental Engineering (CEE), University of Strathclyde.

A Metrohm 850 Professional ion chromatographer was used for determination of five anions (F^-, Cl^-, SO_4^{2-}, Br^-, NO_3^-). The separation utilised a Metrosep A Supp 5 anion analytical with Guard column (Metrosep A Supp 5 Guard/4.0) at 24°C and an eluent comprising of 1 mM $NaHCO_3$ and 3.2 mM Na_2CO_3 prepared in ultra-pure water (18.2 MΩ cm^{-1}) (Triple Red water purification system). The flow rate was 0.7 ml/min. Calibration standards were 0.1, 0.5, 1, 5 and 10 mg/L and prepared in ultra-pure water. Samples with elevated concentrations were diluted with ultra-pure water to a level within a calibration range. Anion concentration was chosen on an individual basis, when the least diluted sample version fitted the calibration range. The ion chromatography (IC) method was developed according to British Standards Institution (2009) and Metrohm customer support recommendations.

Determination of 12 dissolved and total elements (B, Ba, Ca, Fe, K, Mg, Mn, Na, S, Si, Sr and Zn) used an Inductively Coupled Plasma Optical Emission Spectrometer (ICP-OES) iCAP 6,200 Duo View ICP Spectrometer, Thermo Fisher Scientific model equipped with an autosampler (Teledyne CETAC Technologies, ASX-520) and Thermo i-TEVA Version 2.4.0.81, 2010. The operating conditions are presented in **Supplementary Appendix SC**.

For determination of total elemental content, the samples were acid digested using a Microwave Assisted Reaction System (MARS-6, CEM). 10 ml of thoroughly mixed, unfiltered sample was transferred into MARS Xpress Plus 110 ml Perfluoroalkoxy alkane (PFA) microwave digestion vessels. Samples were digested with reversed "*Aqua Regia*" mixture of hydrochloric and nitric acids (1:4, HCL −37%, and HNO_3 −68%, Trace Metal Grade, Fisher Chemicals). The following microwave operating parameters were utilised: maximum power −1,800 W; ramp time −20 min; hold time -20 min; temperature −170°C. Sample digests were brought up to 50 ml with ultrapure water using volumetric flasks, then filtered through 0.45 µm for ICP-OES analyses.

Multi-element 3-point calibration standards were prepared from 1,000 mg/L element stock standard solutions (Fisher Scientific) using ultrapure water. Addition of 68% trace metal analysis grade nitric acid (Fisher Chemicals) to a final acid concentration of 5% for dissolved content analyses, and addition of reversed "*Aqua Regia*" to 20% for total elemental content analyses. Yttrium (5 mg/L) was used as an internal standard (IS) solution (Fisher Chemicals), to account for any matrix effects due to differences between samples and standards. The IS was added through automated online addition with an internal standard mixing kit. A brief method validation study found the following linear ranges: 0.01–1 mg/L for barium and strontium, 0.5–50 mg/L for calcium, magnesium, potassium, sodium, iron and sulphur and 0.1–10 mg/L for boron, manganese, silica and zinc. Analyses proceeded when calibration curves generated correlation coefficients (R^2) >0.9980. Instrument equilibration and system's suitability were checked according to CEE labs Standard Operating Procedure for

ICP-OES and Quality Control and Assurance procedure. CEE methods of analyses were mainly based on British Standards Institution (2018).

Elemental method quantification limits were based on instrument-predicted method quantification limit values (**Supplementary Appendix SC**), obtained from the calibration parameters for each element.

In addition to field analyses of alkalinity, the decanted portion of the anion aliquot was analysed for laboratory-based alkalinity using an automated discreet KoneLab Aqua 30 (Thermo Scientific Aquarem 300; Clinical Diagnostic). Methyl orange buffer solution approach was used, with the intensity of colour measured spectrophotometrically at 550 nm. All relevant data is included in **Supplementary Appendix SB**.

Laboratory Isotopic Analytical Methods

Isotopic determinations for all 57 sampled mine water discharges were carried out at the National Environmental Research Centre (NERC) National Environmental Isotope Facility (NEIF) Stable Isotope Laboratory based at the Scottish Universities Environmental Research Centre (SUERC), East Kilbride.

For $\delta^{18}O$ analysis, samples were over-gassed with a 1% CO_2-in-He mixture for 5 min and left to equilibrate for a further 24 h. A sample volume of 2 ml was then analysed using standard techniques on a Thermo Scientific Delta V mass spectrometer set at 25˚C. Final $\delta^{18}O$ values were produced using the method established by Nelson (2000). For $\delta^{2}H$ analysis, sample and standard waters were injected directly into a chromium furnace at 800˚C (Donnelly et al., 2001), with the evolved H_2 gas analysed on-line *via* a VG Optima mass spectrometer. Final values for $\delta^{18}O$ and $\delta^{2}H$ are reported as per mille (‰) variations from the V-SMOW standard in standard delta notation. In-run repeat analyses of water standards (international standards V-SMOW and GISP, and internal standard Lt Std) gave a reproducibility better than ±0.3‰ for $\delta^{18}O$ and ±3‰ for $\delta^{2}H$. For sulphate-$\delta^{34}S$ isotope analysis, barium sulphate precipitate was recovered from the sampling vessel, washed repeatedly in deionised water and dried. SO_2 gas was liberated from each sample by combustion at 1,120˚C with excess Cu_2O and silica, using the technique of Coleman and Moore (1978), before measurement on a VG Isotech SIRA II mass spectrometer. Results are reported as per mille (‰) variations from the Vienna Canyon Diablo Troilite (V-CDT) standard in standard delta notation. Reproducibility of the technique based on repeat analyses of the NBS-127 standard was better than ±0.3‰.

Quality Assurance

The ion balance errors (IBE) were deemed acceptable after they returned 31 results within ±5%, 20 within ±10%, 5 within ±15%, and one outlier at 17%. Despite the outlier having an IBE of 17%, the disparity between cations and anions was 0.23 meq/L, reflecting a very low margin for error for samples with low mineralisation.

Since sulphate (SO_4^{2-}) was run *via* IC, and sulphur elemental analysis was run *via* ICP-OES, correlation between the two for sulphate (meq/L) is possible (on the assumption that all sulphur is present as sulphate). These show a very strong correlation (**Supplementary Appendix SC**), but sulphate concentrations derived from measured ICP sulphur were selected for use in IBE and presentation. The correlation between field and laboratory alkalinity was good (**Supplementary Appendix SC**). The laboratory analyses are preferred and cited since a colorimetric endpoint was sometimes difficult to judge in the field for mine waters tinted with turbidity, iron flocs or changing daylight.

"Field blanks" were collected in parallel to discharge samples, ultrapure water was carried into the field and analysed subject to the same collection and processing methods as the discharge samples, e.g., filtration, acidification, digestion. This was done to monitor for any contamination of samples during collection. Laboratory blanks were created from ultrapure water and subjected to the same laboratory processes as the discharge samples to check for contamination. All field and lab blanks returned acceptable values which concluded there was no, or minimal interference from the process of field sampling, sample preparation and/or laboratory analyses.

Thermal Resource Estimates

The thermal resource potential of discrete mine water flows present at the surface was calculated using two different methods. Firstly, as a function of flow rate and temperature, the heat available (G) was calculated in **Eq. 3**.

$$G = Q \cdot \Delta T \cdot S_{VCwat} \quad (3)$$

where, Q is flow rate (L/s), ΔT is temperature change in K, S_{VCwat} is volumetric heat capacity of water (4180 J L^{-1} K^{-1}). The ΔT value is the temperature change in the mine water that can be effected by a heat exchange or heat pump device and will also depend on the raw temperature of the mine water. For G, the ΔT will vary since the warmer the source water, the greater the temperature drop that can be accomplished without risk of freezing in the heat exchanger. We selected 6˚C as a suitable return temperature following heat exchange, therefore, ΔT values are defined as the difference between the mine water temperature and the postulated return temperature of the "thermally spent" mine water (6˚C). Note that absolute temperature values e.g., discharge source or return temperatures, are in ˚C, whereas relative temperatures and changes (ΔT), for use in equations, are in K.

Alternatively, we can estimate the total heat pump delivery (H) (**Eq. 4**) from a heat pump system, the principal differences being that: 1) additional heating is added from the electrical input of the heat pump, and 2) the value of ΔT is set at an assumed constant value of 4 K (as opposed to fluctuating with source temperature). We assumed a uniform coefficient of performance (COP) of 4, though it should be noted that heat pump COP can vary depending on the temperature of the heat source. The only variable for H in **Eq. 4** is flow rate (Q), therefore

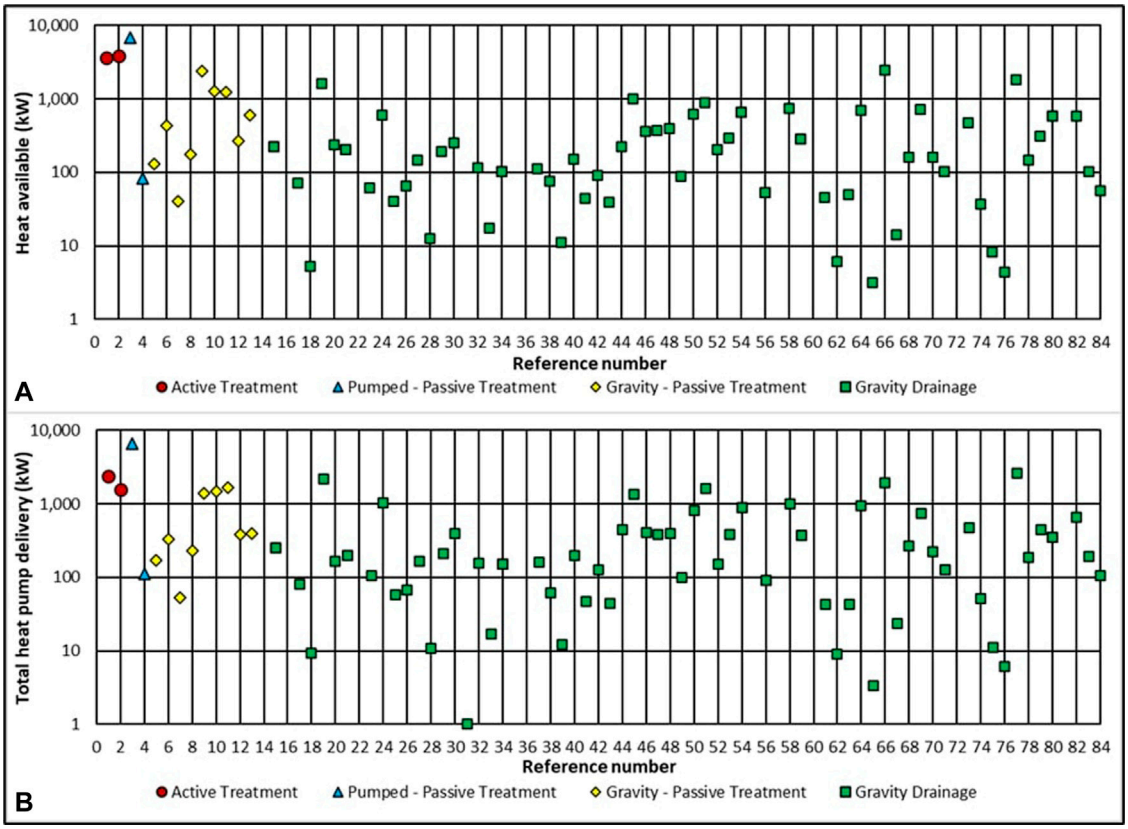

FIGURE 2 | Thermal outputs of treatment sites and gravity drainages. Heat available **(A)** and total heat pump delivery **(B)**.

resources with high temperatures do not generate higher values, as they would for G.

$$H = \frac{Q \cdot \Delta T \cdot S_{VCwat}}{1 - \left(\frac{1}{COP}\right)} \quad (4)$$

It should be noted that, while a small ΔT of 4 K is a reasonably typical figure for a heat pump evaporator, larger ΔT values can be achieved by manipulating flow rates across a secondary heat exchanger, although larger ΔT will typically be at the expense of COP.

RESULTS AND DISCUSSION—THERMAL RESOURCES

A catalogue of discharge descriptions and images is available in the supporting material **Supplementary Appendices SA,B**. Since the original mine discharge data was 2 decades old, it was clear that in some instances, more recent developments had altered the presence or form of the discharges. Some locations had treatment sites established by TCA, whilst others were near new housing developments, where shallow mine voids may have been thoroughly grouted for ground stability.

Heat available (G) from each of the locations of the discharges or treatment sites is plotted in **Figures 1**, **2**. The greatest single source of mine water heat available at the surface is 6.9 MW (Blindwells - pumped, passive treatment site - #3). With a source temperature of 11.6˚C (ΔT = 5.6 K), and an average discharge of 294.6 L/s (Bailey et al., 2016), Blindwells hosts the highest available surface mine water heating resource in Scotland. The two Coal Authority sites with pumping and active treatment (Frances - #1; Polkemmet - #2), host the next highest values of available heat, 3.6 MW and 3.9 MW respectively. One treatment site with gravity drainage and passive treatment has a heating capacity over 2 MW (Minto - #9), whilst two others of the same nature host available heat above 1 MW (Pitfirrane - #10; Pool Farm - #11).

The potential heating resource of treatment or pumping stations is already understood by TCA (Bailey et al., 2016), where 34 billion litres of water was treated by TCA in Scotland during 2020–2021 (The Coal Authority, 2021). The total estimated volume of water across the year equates to c. 1078 L/s estimated flow rate, which when used for total heat pump delivery (H) (**Eq. 4**), with a ΔT value of 4 K and a COP of 4 gives a total potential heat delivery of:

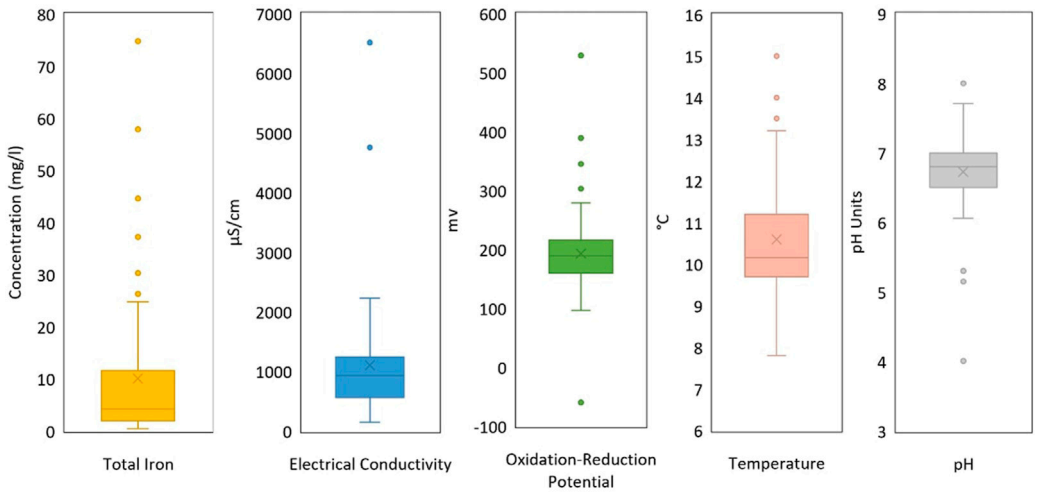

FIGURE 3 | Box and whisker plots for total iron and physicochemical properties for all gravity drainages in Scotland including those treated by TCA (Bailey et al., 2016) or the council (James Hutton Institute, 2016), and the untreated discharges sampled in this study.

$$H = \frac{1078\,L\,s^{-1} \cdot 4\,K \cdot 4180\,J\,L^{-1}\,K^{-1}}{1-\left(\frac{1}{4}\right)} \quad (5)$$

$$H = 24\,MW$$

Combining temperature and flow rate data from other sources (Whitworth et al., 2012; Bailey et al., 2016; James Hutton Institute, 2016), suggest that the total heat pump delivery (H) from treatment sites across Scotland (TCA and Council operated) is a more modest 16.8 MW, from a total flow rate of 754 L/s. Heat available (G) (**Eq. 3**) derived from the same dataset for the Scottish treatment sites produces a higher overall total of 21 MW since this reflects larger ΔT values than the standard 4 K for H (in some cases ΔT is as high as 13.2 K from a discharge temperature of 19.2°C (Polkemmet, #2)), however the additional heating contribution from the heat pump is absent.

In addition to TCA pumping or treatment sites, the untreated gravity drainages found as part of this study are estimated to have a collective total heat pump delivery (H) (with ΔT value of 4 K and a COP of 4) of 23.9 MW, which doubles potential heat delivery from surface mine water in Scotland. Heat available (G) from untreated gravity drainages is 19.3 MW. Untreated discharges reported in (Whitworth et al., 2012) which feature in **Supplementary Appendix SA** (i.e., not sampled in this study) were assigned a temperature of 10°C, and therefore the true value for G may be slightly higher.

Treated and untreated mine water combine to present a heating potential of up to c. 48 MW available at the surface. Surface resources provide the 'lowest hanging fruit' when planning mine water heating and cooling development. These resources can be harnessed without significant capital expenditure for drilling and with greatly reduced pumping costs as part of the operational expenditure. Visualising heat units (W - watts) can be simplified by assigning an average 2 bed house/flat a thermal peak demand of 4 kW (BoilerGuide, 2022). With this generalised assumption, we can state that up to 12,000 two bedroom homes could be heated by surface mine water resources. This optimistic viewpoint should be tempered by the fact that many of the discharges are distant from urban areas and other loci of heat demand, meaning that the potential thermal resource has no obvious user at present. Prior to harnessing the thermal energy of a mine water discharge, regular sampling and monitoring should be performed to establish environmental baselines and seasonal temperature variability. These data are imperative for assessing overall heating/cooling delivery before installation of any associated infrastructure.

RESULTS AND DISCUSSION—HYDROCHEMICAL DATA

Physicochemical Properties

The physicochemical results for every gravity drainage (#5-84) including those treated by TCA (Bailey et al., 2016) or local council (James Hutton Institute, 2016) are presented as box and whisker plots in **Figure 3** and listed in **Table 3**. The box portion contains the middle 50% of the data points (between the 25th and 75th percentiles), representing the interquartile range (IQR) (Tukey, 1977). The central line represents the median value, whilst the cross locates the arithmetic mean. The "T" shaped whiskers extend towards the maximum and minimum values of the dataset. Their extent is capped at 1.5 times the length of the box (Reimann et al., 2008), and reach as far as the most extreme value within this range. Beyond the extent of the whiskers, individual extreme outlier data points are plotted. Any samples with values below detection limits have been set to 0 for the purposes of plotting.

TABLE 3 | Results for all gravity mine drainages (not including the 4 pumped systems in Scotland). Data from TCA treated discharges available only for: Flow rate, Temperature, Heat Available, Total Heat Delivery with COP of 4 and ΔT = 4 K, pH, Electrical Conductivity, Alkalinity and Fe (total).

		Units	Maximum	75th percentile	Median	Mean	25th percentile	Minimum
Field data	Flowrate	L/s	117	20.0	8.93	19.5	3.0	0.15
	Temperature	˚C	15.1	11.2	10.2	10.6	9.70	7.80
	pH	pH units	8.00	6.99	6.80	6.73	6.52	4.01
	Electrical Conductivity	µS/cm	6,515	1,238	932	1,104	578	146
	Oxidation-Reduction Potential	mV	330	14	−10	−3	−39	−103
	Alkalinity	meq/L	22.1	8.43	5.45	6.26	3.02	0
Calculated thermal potentials	Heat Available (G)	kW	2,487	426	154	358	50.7	0.71
	Total heat pump delivery (H)	kW	2,606	438	197	429	63.5	1.00
Laboratory chemical data	F^-	mg/L	0.620	0.147	0.116	0.143	0.093	0.060
	Cl^-	mg/L	900	43.7	30.5	65.6	17.9	7.31
	SO_4^{2-}	mg/L	1,170	250	148	223	72.7	6.71
	Br^-	mg/L	13.1	3.16	1.26	1.92	0.354	>0.02
	NO_3^-	mg/L	11.6	1.03	0.215	1.10	0.022	>0.01
	Na	mg/L	1,345	44.9	23.9	69.4	16.0	4.36
	Ca	mg/L	256	121	94.7	97.5	54.7	5.10
	Mg	mg/L	158	63.0	40.7	47.3	22.2	2.38
	K	mg/L	38.3	14.5	7.48	9.87	3.87	0.830
	Fe (total)	mg/L	74.8	11.2	4.23	10.1	1.98	0.416
	Fe (Diss)	mg/L	56.0	7.30	3.41	8.64	1.52	0.024
	Mn (Total)	mg/L	6.61	1.63	0.770	1.31	0.371	0.030
	Mn (Diss)	mg/L	6.72	1.76	0.853	1.43	0.499	0.013
	Sr	mg/L	3.04	1.36	0.616	0.89	0.243	0.016
	Si	mg/L	14.7	6.73	4.75	5.73	4.09	2.06
	B	mg/L	0.838	0.152	0.074	0.140	0.032	0.002
	Zn	mg/L	0.194	0.024	0.008	0.021	0.004	0.001
	Ba	mg/L	0.231	0.071	0.039	0.054	0.026	0.013
Chemical ratios	Cl/Br mass ratio		1904	98.6	26.1	125.0	10.8	2.42
	SO_4^{2-}/Cl^- molar ratio		16.72	3.22	1.61	2.74	0.655	0.080
	Na/Cl^- molar ratio		11.97	1.43	1.06	1.88	0.902	0.426
	$(Ca + Mg)/SO_4^{2-}$ meq ratio		16.8	3.72	2.51	3.11	1.45	0.525
	Ca/Mg molar ratio		7.32	1.717	1.340	1.601	1.036	0.752
	Ca/Alkalinity meq ratio		1879	1.28	0.760	35.1	0.591	0.242
Laboratory isotopic data	$\delta^{34}S_{vCDT}$	per mille	+48.0	+13.3	+9.9	+10.7	+5.3	+0.3
	$\delta^{18}O_{vsmow}$	per mille	−6.8	−7.4	−7.6	−7.6	−7.8	−8.5
	$\delta^{2}H_{vsmow}$	per mille	−43.7	−48.0	−49.2	−49.6	−52.0	−57.0

Water temperatures range between 7.8˚C and 15.1˚C. Very shallow coal mine drainages with short groundwater flow pathways can be influenced by thermal variations at surface or percolating rainfall temperatures, causing discharge temperature to fluctuate across the seasons (Farr et al., 2016). Higher temperatures reflect mine water source depth and the geothermal gradient of an area (Farr et al., 2021), buffered from surface temperature fluctuations by tens to hundreds of metres of bedrock. The highest overall discharge temperature is from TCA's treatment site at Minto (#9) gravity drainage (15.1˚C) (56.1391˚N, 3.2808˚W) where the coordinates of the discharge location correlate with the disused No.1 and No.2 shafts of Minto Colliery, reaching 184 m BGL and 302 m BGL respectively (The Coal Authority, 2022). The highest temperature discharge sampled as part of this study (15.0˚C) is Wallyford Great (55.9475˚N, 3.0167˚W) (#80). Watson (2007) explains the arrangement of the Wallyford Great 'engineered' discharge, which flows from an artesian borehole. The borehole was recently drilled (in 2005) to c. 190 m BGL, where it is understood to drain artesian waters from unrecorded limestone workings, connected to Wallyford colliery. Temperature seasonality was not measured in this study, but accounts of mine water discharges from Wales in Farr et al. (2016) show a variety of temperature responses throughout the year. Deep sources demonstrated greater stability (subset reported in Walls et al. (2021)), whilst shallow sources or rapidly recharging systems, showed greater temperature fluctuation, some displaying an IQR of around 3˚C (Farr et al., 2016).

Electrical conductivity (EC) ranges between 146 µS/cm and 6,515 µS/cm, with an interquartile range of 564–1,242 µS/cm. EC reflects total ionic solute content and is influenced by groundwater residence time, influence of marine or connate water, soil zone processes (e.g., rainfall evapotranspiration and CO_2 generation), rock mineral suite and degree of weathering. In coal mines, one potential determining reaction is sulphide

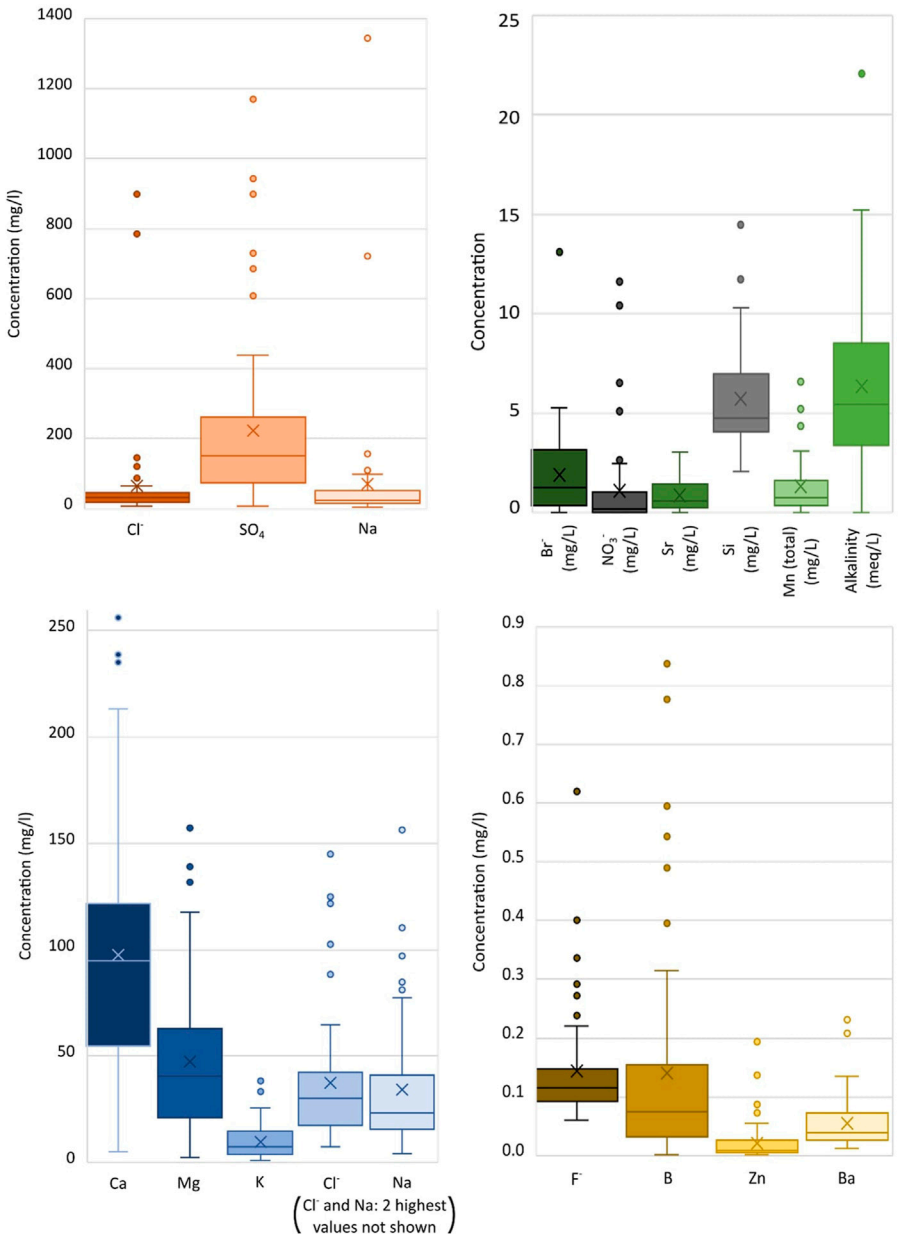

FIGURE 4 | Box and whisker plots following water chemistry analysis of the untreated gravity discharges sampled in this study (not including treated discharges by TCA or council). All values in mg/L except alkalinity in meq/L.

oxidation which not only releases iron and sulphate, but also protons, which hydrolyse other minerals and release base cations and alkalinity. Consumption of protons (acid) by carbonate (and silicate) weathering explains the circumneutral pH values observed in many of the mine waters, and their alkalinity content (Wood et al., 1999). However, it is also known that deep coal mines sometimes host naturally saline formation water (Anderson, 1945; Younger et al., 2015). The two elevated EC outliers are Glenburn (#52) (6,515 µS/cm) and Douglas (#39) (4,756 µS/cm). Associated elevated Na and Cl^- values for the Glenburn discharge (55.5145˚N, 4.6223˚W) and an immediate proximity to the coast, reasonably suggests marine influence on chemistry and EC. The Douglas discharge (55.6008˚N, 3.7994˚W) also contains elevated Na and Cl^- values but is sited c. 50 km from the coast. The recorded mine adit appears to drain workings associated with Douglas colliery's main shafts (both 238 m deep (Oglethorpe, 2006)) and to be overlain by spoil heaps (bings) from the mine. It is known that deep mines throughout the UK are characterised by highly saline formation waters (Younger et al., 2015). The sodium chloride content in the Douglas mine water (721 mg/L sodium and 900 mg/L chloride) could thus be due to a component of saline water either in the mine water itself or in leachate from the spoil tips percolating into the adit.

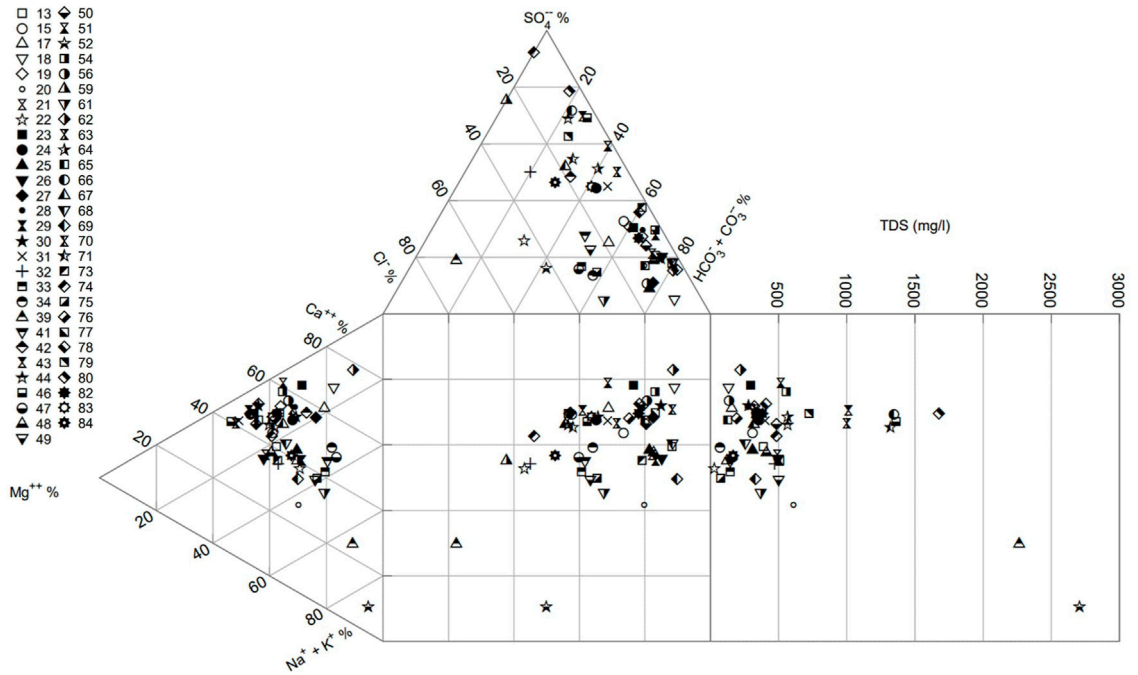

FIGURE 5 | Durov plot for untreated gravity discharges sampled in this study, with total dissolved solids (TDS) shown on right hand extension plot.

Highly variable redox conditions in shallow mine waters are reflected by ORP ranges between −103 mV and +330 mV, with a median value just below zero (−10 mV). 23 of 58 discharges (39.7%), not including those treated by TCA, had an H_2S odour.

Total iron present in Scotland's mine water discharges ranges from 0.4 mg/L to 74.8 mg/L, with an interquartile range of 2.0–11.6 mg/L. The Dalquharran (#5) discharge (55.2799˚N, 4.7308˚W) hosts the highest total iron concentration, after infamously having one of the highest ever recorded peak iron concentrations (c. 1,500 mg/L) during the "first flush" phase of mine water rebound and surface breakout (Younger and Adams, 1999). Peak and long-term iron concentration are often linked and may correlate with total sulphur content of the worked coal seams (Younger, 2000b). The Dalquharran discharge is currently intercepted by a passive treatment arrangement operated by TCA, before outflow to the local watercourse (Water of Girvan).

Elemental Properties

The following figures and hydrochemical interpretations consider only the 57 sample sites of this study. TCA treatment sites have been omitted since they are partially characterised elsewhere (Bailey et al., 2016), and sampling access was limited. **Figure 4** shows box and whisker diagrams for mine water chemistry. Bicarbonate and sulphate are the dominant anions in the mine water. Chloride is a dominant anion in two discharges (discussed above). Elevated sulphate in the mine waters is usually assumed to reflect the products of sulphide oxidation processes, but interpretation of $\delta^{34}S$ may also suggest other possible sulphate sources including marine inundation, evaporites, evaporitic brines or carbonate associated sulphate (CAS).

The most common mine water type is calcium-bicarbonate. Calcium is the dominant cation for 18 of the 57 samples (>50% meq/l contribution) and for a further 23 samples is the highest percentage (meq/l) cation. Bicarbonate is the dominant anion in 34 of the 57 samples (>50% meq/l contribution) and has the highest percentage (meq/l) for another 2 samples. 18 of the sampled waters have sulphate as the highest percentage anion (in meq/l). A Durov plot with total dissolved solid (TDS) concentration is shown in **Figure 5**. Cation meq/L values mostly cluster in an area around 35%–65% Ca, 15%–55% Mg and 0%–40% Na + K, with a few outliers more dominated by Ca or Na. Anion meq/L plots spread between sulphate and alkalinity, with the majority <20% Cl. There is a slightly higher density skewed towards higher percentages of alkalinity. The central plot suggests that, when excluding the high concentration saline outliers, greater TDS values correlate with sulphate-dominated anion balances.

The Younger diagram (**Figure 6**) was designed to plot groundwaters which have been affected by pyrite oxidation and to interpret their source and history (Younger, 2007). Plotting Younger diagrams requires total acidity. This is calculated using the method outlined in (Younger, 2007) whereby total acidity in meq/L is defined as:

$$Total\ Acidity = 1000\left(10^{-pH}\right) + \left\{Fe^{2+}\right\} + \left\{Fe^{3+}\right\} + \left\{Mn^{2+}\right\} + \left\{Zn^{2+}\right\} + \left\{Al^{3+}\right\} + \left\{Cu^{2+}\right\} \quad (6)$$

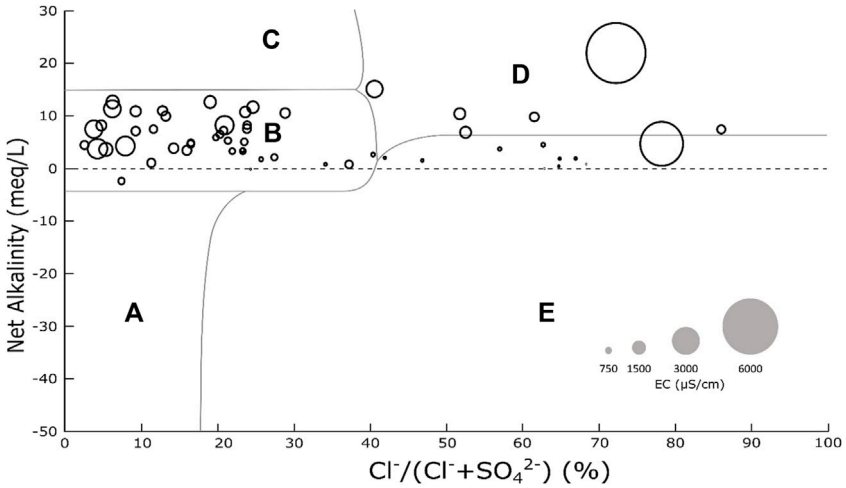

FIGURE 6 | Younger diagram with untreated discharges from this study, where bubble sizes reflect the EC value. The Cl^- and SO_4^{2-} on the x-axis are both meq/L. The typical plotting fields are: **(A)**—Acidic spoil leachates, tailings/bing drainage, and shallow oxygenated workings in pyrite rich strata; **(B)**—Majority of fresh, shallow, ferruginous coal mine waters; **(C)**—Previously acidic waters, since neutralised; **(D)**—Deep-sourced pumped, saline mine waters; **(E)**—Field in which few mine waters plot.

TABLE 4 | Total iron loading of mine water into Scottish treatment sites based on total iron concentrations.

Treatment site	Type	Flowrate (L/s)	Total iron (mg/L)	Iron loading (Kg/Day)
Frances	Active Treatment	109	57.1	537
Polkemmet	Active Treatment	70	24.7	149
Blindwells	Pumped - Passive Treatment	295	4.4	112
Cuthill	Pumped - Passive Treatment	5	24.5	10.6
Median from Gravity Passive Treatment (n = 9)		17.0	11.9	23.3

Where each of the values in parentheses is the concentration of the dissolved ion in meq/L. To make this calculation, it is assumed that the dissolved iron in the water is in ferrous form (ferric iron is generally insoluble in all but the most acidic waters). The main mineral contributors to acidity are almost exclusively ferrous iron and manganese.

Net alkalinity has been plotted on the Y-axis by subtracting the total acidity from the total alkalinity (both in meq/L). The majority of the mine waters plot in field B, i.e., "typical" British coal mine waters, whose chemistry is assumed to be controlled by the processes of pyrite oxidation and neutralisation. For comparison to the X-axis plots, average seawater has a $Cl^-/(Cl^-/SO_4^{2-})$ value of 90.7% (Lenntech, 2022), infiltrating rainfall is 85.4% (O Dochartaigh et al., 2011), and mean values for groundwater from Carboniferous aquifers which have not been extensively mined for coal plot at 56.4% (Ó Dochartaigh et al., 2015). This diagram was created for understanding mine waters but is less useful when plotting waters with low mineralisation (i.e., waters not affected by pyrite oxidation), plotting the conductivities of the discharges as circle sizes shows the low EC samples (small circles) which may not be best characterised by a Younger diagram. In the instance where there is a distinct saline influence on the mine waters (#39; #52), the $Cl^-/(Cl^-/SO_4^{2-})$ ratio increases, despite both having sulphate concentrations in the highest 25% (335.9 mg/L and 405.1 mg/L respectively).

Iron Loading

The iron loading value (kg/day) of a mine water discharge is a function of flow rate (L/s) and total iron concentration (mg/L). The mine waters entering Scottish treatment sites have a combined iron loading of 1,032 kg/day (Bailey et al., 2016; James Hutton Institute, 2016). The mine water is intercepted and treated to remove most of the total iron (**Table 4**) and as a result, the treatment sites prevent 960 tonnes of iron (solids) from entering Scottish water courses each year (The Coal Authority, 2021). The discharges sampled in this study show a combined iron loading of 595 kg/day. Since these discharges are yet untreated, the total iron content currently flows, without interception, into streams and rivers or directly into the ocean. **Table 5** shows the top seven untreated discharges ranked in order of iron loading. They have iron loadings close to or significantly above the median values of the gravity passive treatment sites (**Table 4**), hence a treatment site may become necessary for each of them. Importantly, since flow rate has a positive correlation with both iron loading and heat available (G),

TABLE 5 | Correlation of iron loading and heat available for the untreated discharges with the highest iron loadings, based on total iron concentrations.

Discharge	Flowrate (L/s)	Total iron (mg/L)	Iron loading (Kg/Day)	Heat available (MW)
Old Fordell	88	26.8	202	2.49
Marnock	43	26.7	98.9	0.70
Wallyford Great	16	44.6	60.6	0.59
Falkirk	20	26.3	45.4	0.22
Shotts	117	2.5	25.5	1.81
Boghead	46	5.1	20.3	0.60
Barbauchlaw	99	2.0	17.0	1.61

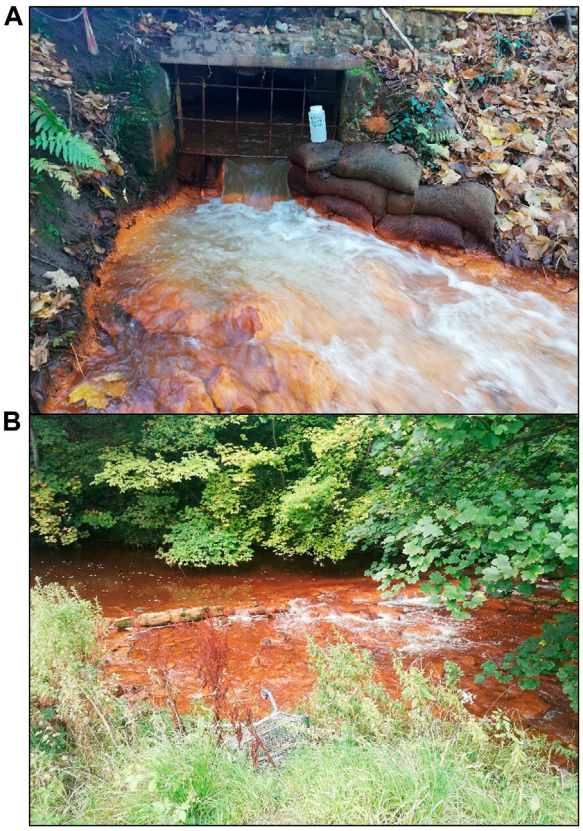

FIGURE 7 | Images of Old Fordell ("Junkie's Adit") mine water discharge **(A)**, which hosts the highest iron loading of the untreated discharges (1L bottle for scale), and the resulting downstream ochre precipitation on the River South Esk **(B)**.

the discharges with the highest iron loadings represent high heating potential. **Table 5** shows that six of the seven highest iron loadings have greater than 0.5 MW heat available, with the greatest at Old Fordell (Junkie's Adit: #66) on the River South Esk having 2.49 MW. Old Fordell causes extensive ochre smothering along the river in the centre of Dalkeith, Midlothian (**Figure 7**). There is reason therefore, for future mine water treatment systems to incorporate a means to harness and distribute the heating capacity of the mine water discharges.

Stable Isotope Data

O and H

O and H isotopic values for discharges of this study (outlined in **Supplementary Appendix SB**) are plotted in **Figure 8**. The results from the University of Glasgow meteoric control samples (**Supplementary Appendix SD**) are plotted alongside, with their trendline generating the mean Local Meteoric Water Line (LMWL). All the mine discharge samples plot close to the mean Global Meteoric Water Line (GMWL) and the LMWL. The arithmetic means for the mine water discharges (**Figure 8**) ($\delta^{18}O$ = −7.6; $\delta^{2}H$ = −51) overlap within one standard deviation of the arithmetic means for the meteoric controls ($\delta^{18}O$ = −7.2; $\delta^{2}H$ = −48). This demonstrates that the mine waters' H_2O component is likely derived from relatively recent meteoric water and has not undergone significant isotope exchange with minerals or evaporative processes: thus, no trace of deep, interacted, more ancient groundwaters are detected.

S Isotopes

A histogram with sulphur isotope $\delta^{34}S$ values for the gravity drainages sampled in this study show a range between 0‰ and +48‰ (**Figure 9**). 52 of the 56 measurements plot between 1‰ and 20‰, but without a clear mode. The factors controlling the sulphate sulphur isotopic composition of the mine waters remains unclear. Banks et al. (2020) suggested that high $\delta^{34}S$ (around or above +20‰) might reflect a contribution from marine-derived salts (although elevated chloride would distinguish these), from evaporite dissolution in overlying or adjacent strata (however this might be reflected by elevated Cl^-/Br^- ratios if halite was present), or from residual evaporitic brines. They also suggested that sulphate reduction processes might serve to elevate mine water $\delta^{34}S$ in some cases.

The dominant signature of the mine waters has $\delta^{34}S$ between +2‰ and +20‰ (**Figure 9**). Typical Coal Measures pyrite values range from -26.3‰ and +18.4‰ (Bullock et al., 2018), thus, the majority of mine water $\delta^{34}S$ are at least compatible with the hypothesis of predominant sulphide oxidation derivation. However, there is a disparity between the distributions of the two sample groups. The Coal Measure pyrite values have a mean of +2.7‰ (Bullock et al., 2018), whilst the mine waters show a heavier mean $\delta^{34}S$ value of +10.7‰ and have no samples with negative $\delta^{34}S$, suggesting there remains isotopically heavy sulphate entering the system adding to the value expected from oxidation of pyrite minerals.

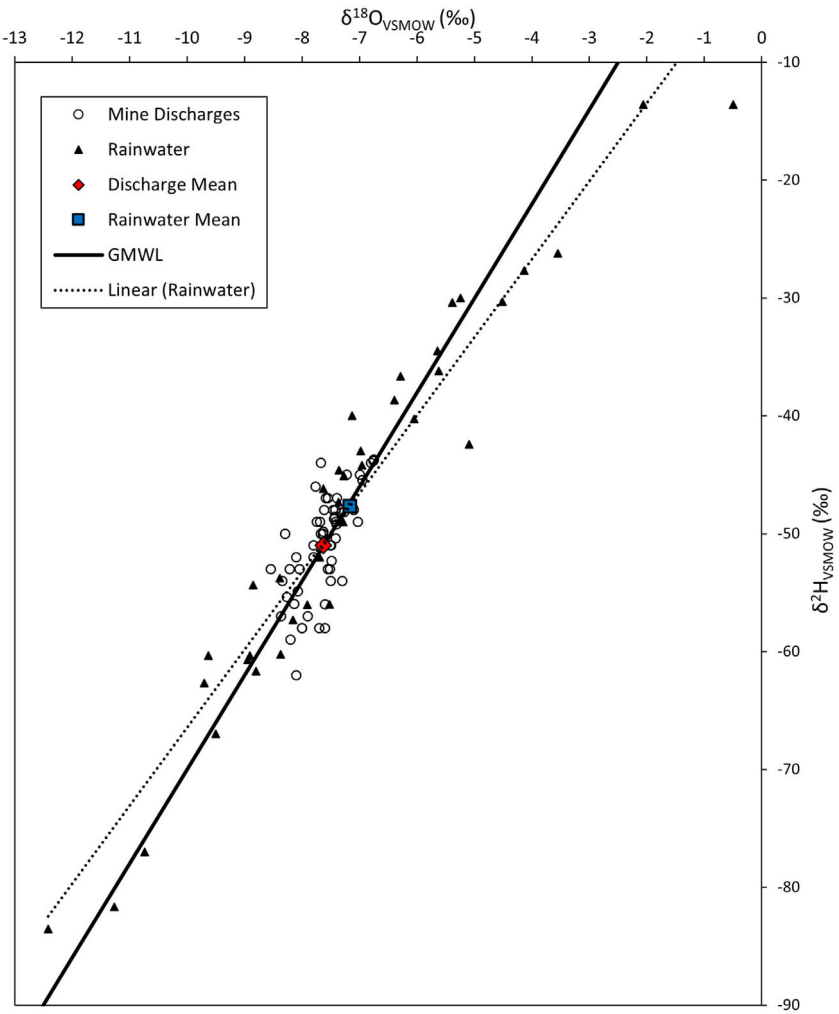

FIGURE 8 | Oxygen and hydrogen isotope plot for the untreated MVS mine water discharges against the global meteoric water line (solid) and a local meteoric water line (dashed) derived from rainwater samples at the University of Glasgow.

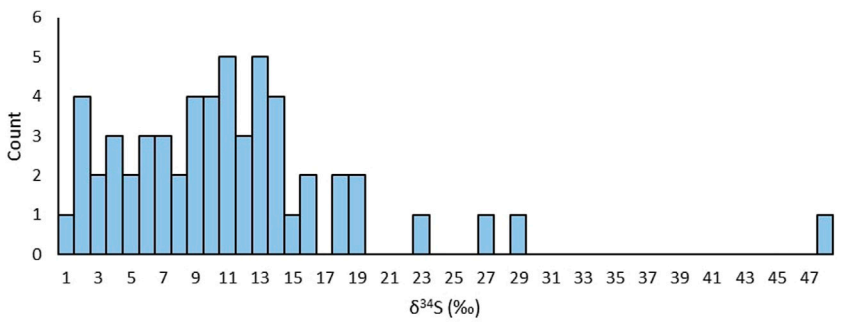

FIGURE 9 | Histogram of $\delta^{34}S$ values collected from the untreated mine water discharges in this study.

Scottish contaminated mine drainages' (CMD) neutrality is ascribed to a pH buffering effect caused by dissolution of carbonate minerals in the host rocks as outlined above (Farr et al., 2016; O Dochartaigh et al., 2011; Wood et al., 1999). Resulting groundwaters have increased (and in many cases, dominant) concentrations of hardness minerals (Ca and Mg)

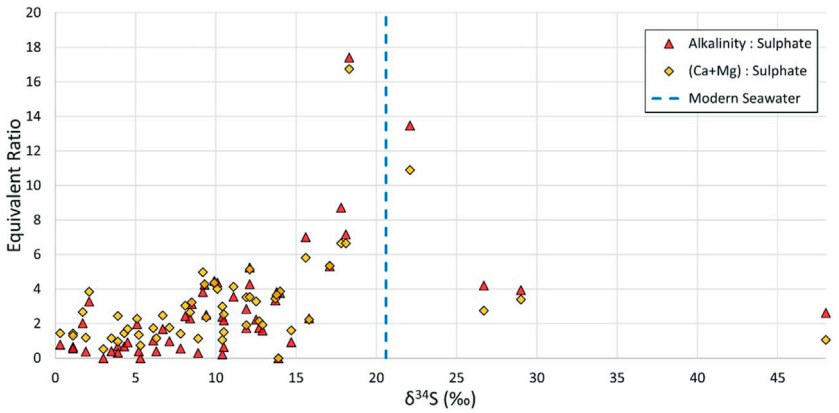

FIGURE 10 | $\delta^{34}S$ plots against alkalinity to sulphate ratio, and calcium and magnesium (combined) to sulphate ratio (both as meq/L ratios).

and alkalinity. A Limestone Coal Formation core sample from the British Geological Survey's (BGS) Glasgow Geothermal Energy Research Field Site (GGERFS) shows elemental calcium and magnesium present at average concentrations of 12,700 ppm (1.27%) and 6,928 ppm (0.69%) respectively from X-ray Fluorescence (XRF) readings at 2 cm intervals across 168 m of bedrock (Monaghan et al., 2021). The median value for the Ca/alkalinity ratio of the mine water discharges is close to one, suggesting that calcite dissolution is a predominant source of Ca and alkalinity to the water. Evidence from these sources shows that carbonate minerals are present throughout coal bearing rocks, found most densely in marine (fossiliferous) limestone units and tidal deposited mudstones with a range of biotic fossil remains (Monaghan et al., 2021).

Figure 10 shows that an increase in the equivalent ratios of alkalinity or Ca and Mg versus sulphate correlate somewhat with increasing $\delta^{34}S$ values between zero and the quoted $\delta^{34}S$ value for Namurian and Westphalian seawater (c. +14‰ and +16‰), and beyond towards modern seawater (+21.2‰) (Tostevin et al., 2014). Carbonate associated sulphate (CAS) in limestones and marine bands host $\delta^{34}S$ values reflective of Carboniferous seawater (Wu et al., 2014) and, given the evidence for extensive carbonate dissolution could reasonably be a factor explaining the heavier $\delta^{34}S$ in discharge waters. Where mine waters contain sulphate sourced only from oxidised coal seam pyrites the ratio of alkalinity to sulphate would be expected to be <1. With progressive dissolution of carbonate minerals and incorporation of both alkalinity and CAS, the ratio moves well beyond 1 and, in this study, as high as 17.4. During dissolution of carbonate minerals, the CAS, which is present as structurally substituted sulphate ions within the carbonate lattice (Kampschulte and Strauss, 2004), can be released. However, abundances of CAS in modern biogenic carbonates average around 600 ppm, and in most carbonates around 100 ppm (Fichtner et al., 2017). It is unlikely that heavy $\delta^{34}S$ contribution from CAS could be the sole controlling factor on the groundwater overall $\delta^{34}S$ value, but a potential contribution should not be ignored. If the alkalinity increase relative to sulphate is indicative of sulphate reducing bacteria, often found in anoxic groundwater (Brown et al., 2002), then the CAS hypothesis could be dismissed.

The Banks et al. (2020) hypothesis whereby recent marine inundation leaves a seawater $\delta^{34}S$ footprint (circa +21‰) on the groundwaters can be confidently excluded since chloride concentrations are too low (median = 35 mg/L). The two exceptions to this are Douglas and Glenburn, where the hypothesis may fit since they show elevated salinity. All sampled mine waters have SO_4^{2-}/Cl^- molar ratios which exceed modern seawater (0.052) (Lenntech, 2022) and suggest contribution of sulphate without additional chloride, likely derived from lithological sources (pyrite) (Banks et al., 2020). Likewise, the median Na^+/Cl^- molar ratio is 1.06, (max 12, min 0.43), which exceeds modern seawater (0.858), and suggests some additional lithological sources of sodium (felsic minerals) beyond marine derived salinity (Banks et al., 2020). The Cl^-/Br^- mass ratios of most of the sampled mine waters (median 26.1) show values lower than that of seawater (292) (Lenntech, 2022) (**Figure 11**). The majority also plot lower than typical shallow groundwater ratio values (from 100 to 200) (Davis et al., 1998). Significantly lower values for groundwater, which have reached as low as 4, are attributed to the degradation of humic material in peat deposits (Davis et al., 1998). Organic materials are known to concentrate bromide without concentrating chloride, therefore the authors speculate that overall low Cl^-/Br^- ratios reflect a contribution of bromide from organic matter in coal seams and no additional chloride from marine inundation.

Evaporites of the Ballagan Formation, primarily gypsum with some anhydrite and psuedomorphs of halite, are detailed in Millward et al. (2018), found in abundance amongst fluvial, overbank deposits and saline–hypersaline lake deposits, with the latter hosting the majority of the evaporite minerals. Since the Ballagan Formation is of Tournaisian Age, it correlates with seawater $\delta^{34}S$ values of early Carboniferous at c. +20‰

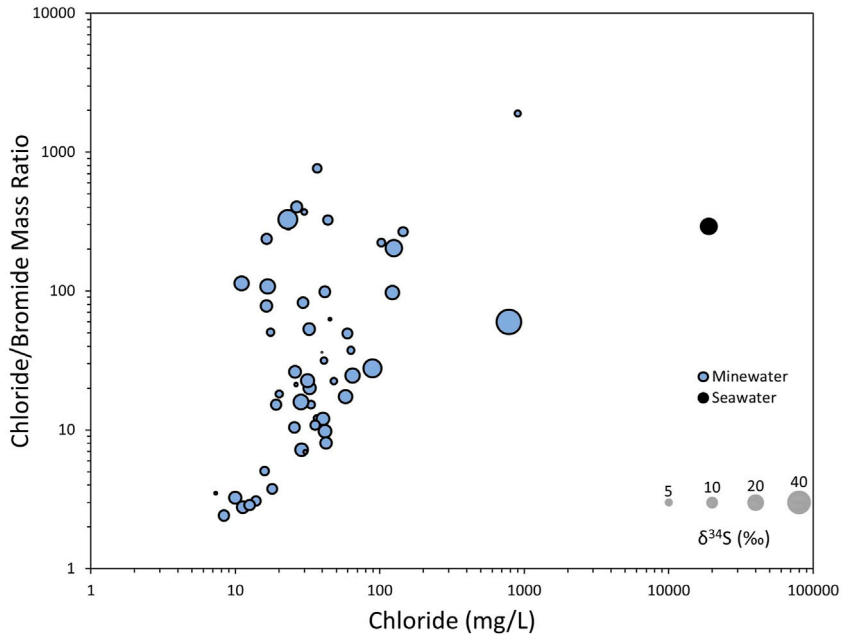

FIGURE 11 | Plot of the chloride: bromide ratio against chloride concentration, with circle sizes proportionate to $\delta^{34}S$ value. Seawater in Black.

(Present et al., 2020), thus dissolution of the sulphate bearing minerals (gypsum and anhydrite) could introduce these heavy isotopic values to the groundwater. Douglas (#39) is the only mine water to have a Cl^-/Br^- above 1,000 (value = 1904), which suggests mixing with a groundwater which has interacted with halite deposits. However, the hypothesis whereby heavy $\delta^{34}S$ values are derived from evaporite mineral dissolution does not fit well with this data since the data points with concentrated Cl^- and high Cl^-/Br^- (especially Douglas) do not show heavy $\delta^{34}S$ values (**Figure 11**). Ca and Mg in the mine water is not consistent with that of SO_4, generating (Ca + Mg)/SO_4 equivalent ratios which range between 0.5 and 16.8, with a median value of 2.5, making gypsum/evaporite dissolution unlikely to be a controlling factor for most of the samples.

Sulphate concentrated in residual saline brines or paleo-evaporites remains a potential explanation for the elevated $\delta^{34}S$ values. Following deposition of the coal bearing strata in the Carboniferous, the MVS created depositional environments for sediments through the Permian to the Cretaceous. Whilst arid desert aeolian conditions dominated in the west through the Permian (Cameron and Stephenson, 1985), the preserved rocks off the coast of the Firth of Forth show evaporite deposits including gypsum and anhydrite from the hypersaline Zechstein Sea (Thomson, 1978). In the late Cretaceous, tropical seas submerged all but the highest areas of Scotland and deposited chalk layers (Harker and Trewin, 2002) during the probable Phanerozoic sea level peak, which may have been 150–300 m higher than present (Rawson, 2006). Arid climates following transgressions may have induced evaporation and concentration of saline waters, leading to brines or evaporites left behind. Whilst the associated rocks have since been eroded (Harker and Trewin, 2002), leaving sparse existing bedrock from the Permian—Cretaceous, the brines may have percolated into the bedrock beneath carrying sulphate with an isotopically heavy seawater/evaporite signature, and, whilst unlikely on geological grounds to be a major source, their contribution cannot be ruled out.

The heavy $\delta^{34}S$ outliers include Glenburn (#52) at +48‰, described for its elevated EC above, is likely influenced by modern seawater, although this would only raise the $\delta^{34}S$ to c. +21‰. The process by which the signature reaches +48‰ is unknown and is far heavier than any value from coal mine water elsewhere. Another very heavy $\delta^{34}S$ value (+29‰) is from Rozelle Park (#75). Whilst Rozelle Park discharge has no recorded mine workings beneath it (The Coal Authority, 2022), the site (55.43896˚N, 4.62201˚W) is underlain by Lower Scottish Coal Measures rocks hosting ironstone seams and thin coals (British Geological Survey, 2008). Small, shallow, unrecorded workings may be present beneath the site and form the source of the 0.5 L/s discharge. The final heavy $\delta^{34}S$ value of +26.7‰ is from the Baron discharge (#20 - 55.7724˚N, 3.9925˚W) believed to be derived from the 32 m deep Broomside-Haugh Shaft (The Coal Authority, 2022) accessing workings of the abandoned Dalziel-Broomside Colliery on the River Clyde, near Motherwell. These samples (Glenburn, Rozelle Park and Baron) are not associated with especially deep mines and would not be expected to exhibit mixing with deep brines or reducing conditions (of the three, only Glenburn had odours of H_2S). There are also no obvious evaporite sources for sulphate in the vicinity of these discharges (and in any case there are no evaporites likely

to have $\delta^{34}S$ higher than around +20‰ for Carboniferous seawater sulphate, e.g., Present et al., 2020). Since the SO_4^{2-}/Cl^- ratios do not suggest current or palaeomarine influence, elevated $\delta^{34}S$ does not support the hypotheses of Banks et al. (2020).

Evidently, the isotopic signature of dissolved sulphate in these mine waters is not homogeneous. Whatever the source of the dissolved sulphate, it is clear that their origin is not from a simple oxidation of pyrite in coals, particularly when considering the significant elevated $\delta^{34}S$ values seen across the MVS. The origin of this sulphate is complex and unpredictable, likely involving the interplay of several sources. This is echoed by the review of Banks et al. (2020), and in Clackmannanshire Scotland which suggests that the signature may indeed be variable *within* any given mine water system (unpublished data).

CONCLUSION

Although mine water chemistry sampled at mine water discharges may not be representative of chemistry at depth in mine systems, this research provides a useful dataset as an entry point for stakeholders looking to install mine water geothermal systems across the Midland Valley of Scotland. Overall, the mine waters are circumneutral with dominant calcium-bicarbonate type, although many have sulphate as the dominant anion. Carbonate (and silicate) minerals are assumed to have been hydrolysed by protons released by oxidation and dissolution of sulphide minerals, in turn releasing base cations and alkalinity. Intriguingly, increasing $\delta^{34}S$ values correlate somewhat with mineralisation from carbonate dissolution. An exclusive origin of sulphate from oxidation of pyrite in exposed coals is unlikely on the basis of the highly variable $\delta^{34}S$ (mostly between 0 and 20‰) which is typically isotopically heavier than source pyrite across the Midland Valley of Scotland: this suggests an interplay of several sources. Inclusion of isotopically heavy sulphate released during the dissolution of marine carbonates is proposed as an influence on the $\delta^{34}S$ values of the mine waters, however its absolute concentrations make it unlikely to be the controlling factor. Marine inundation is unlikely to be the source of heavy isotopic sulphate, but ancient evaporites/evaporitic brines are implicated. The complex origin of the sulphate contrasts with the relatively simple origin of the host water, being dominated by local meteoric water.

Gravity fed or actively pumped drainage from coal mines has been shown to host significant heating potential for circulation in district heating networks if harnessed by heat exchanger technology and converted to useable heat using a heat pump. Using mine water which is present at the surface removes drilling capital expenditure and is less restricted by subsurface risks, however, the discharges are location-dependent, and any heat consumers would have to be proximal. In the Midland Valley of Scotland, the mine water brought to the surface *via* gravity or pumping for treatment has been calculated to provide a total heat pump delivery of 48 MW, corresponding to the peak heating demand of 12,000 two-bedroom houses. Where gravity discharges are not treated by the Coal Authority to remove the dissolved and suspended iron, ochre pollution and smothering reduces natural water quality and oxygen availability in the receiving watercourses. Untreated discharges contribute 595 kg/day of iron to Scottish watercourses and the largest untreated gravity discharge polluters show a strong correlation with high heating potential. The most obvious of these is Old Fordell (Junkie's Adit) in the centre of Dalkeith, Midlothian, which hosts 2.49 MW heating potential. It is thus recommended that any future treatment sites consider installation of heating infrastructure to harness the low-carbon mine water thermal resource, provided a demand exists in the vicinity.

DATA AVAILABILITY STATEMENT

The original contributions presented in the study are included in the article/**Supplementary Material**, further inquiries can be directed to the corresponding author.

AUTHOR CONTRIBUTIONS

Conceptualization, DW, NB, and DB; Methodology, DW, TP, DB, NB, and AB; investigation, DW; Data curation, DW and TP; Writing—original draft preparation, DW; Writing, review and editing, DW, DB, TP, NB, and AB; Supervision, NB, DB, and AB; Funding acquisition, NB. All authors have read and agreed to the published version of the manuscript.

FUNDING

This research was supported by NERC NEIF grant 2301.0920, EPSRC IAA grant EP/R51178X/1 and Energy Technology Partnership Scotland grant PR007-HE. NB is funded by a University of Strathclyde Chancellor's Fellowship. AB is funded by the NERC National Environmental Isotope Facility award at SUERC (NEIF-SUERC, NE/S011587/1) and SUERC.

CONFLICT OF INTEREST

The authors declare that the research was conducted in the absence of any commercial or financial relationships that could be construed as a potential conflict of interest.

ACKNOWLEDGMENTS

We are grateful to the following people for contributing their time to assist with field data collection: Jura MacMillan, Laura

Dozier, Michael Schiltz, Dominic James, David Townsend, and Philippa Wood. We would like to thank landowners who granted access to their land for sampling. We would also like to thank Alison McDonald for her help with isotopic analysis at SUERC.

REFERENCES

Adams, C., Monaghan, A., and Gluyas, J. (2019). Mining for Heat. *Geoscientist* 29 (4), 10–15. doi:10.1144/geosci2019-021

Anderson, W. (1945). On the Chloride Waters of Great Britain. *Geol. Mag.* 82 (6), 267–273. doi:10.1017/S001675680008211X

Andrews, B. J., Cumberpatch, Z. A., Shipton, Z. K., and Lord, R. (2020). Collapse Processes in Abandoned Pillar and Stall Coal Mines: Implications for Shallow Mine Geothermal Energy. *Geothermics* 88, 101904. doi:10.1016/j.geothermics.2020.101904

Bailey, M. T., Moorhouse, A. M. L., and Watson, I. A. (2013). "Heat Extraction from Hypersaline Mine Water at the Dawdon Mine Water Treatment Site," in Proceeding of the Eighth International Seminar on Mine Closure: Cornwall, Cornwall, UK, September 18–20, 2013. Editors M. Tibbett, A. B. Fourie, and C. Digby (Australian Centre for Geomechanics), 559–570.

Bailey, M. T., Gandy, C. J., Watson, I. A., Wyatt, L. M., and Jarvis, A. P. (2016). Heat Recovery Potential of Mine Water Treatment Systems in Great Britain. *Int. J. Coal Geol.* 164, 77–84. doi:10.1016/j.coal.2016.03.007

Banks, S. B., and Banks, D. (2001). Abandoned Mines Drainage: Impact Assessment and Mitigation of Discharges from Coal Mines in the UK. *Eng. Geol.* 60 (1), 31–37. doi:10.1016/S0013-7952(00)00086-7

Banks, D., Younger, P. L., Arnesen, R.-T., Iversen, E. R., and Banks, S. B. (1997). Mine-water Chemistry: the Good, the Bad and the Ugly. *Environ. Geol.* 32 (3), 157–174. doi:10.1007/s002540050204

Banks, D., Athresh, A., Al-Habaibeh, A., and Burnside, N. (2019). Water from Abandoned Mines as a Heat Source: Practical Experiences of Open- and Closed-Loop Strategies, United Kingdom. *Sustain. Water Resour. Manag.* 5 (1), 29–50. doi:10.1007/s40899-017-0094-7

Banks, D., Boyce, A. J., Burnside, N. M., Janson, E., and Roqueñi Gutierrez, N. (2020). On the Common Occurrence of Sulphate with Elevated δ34S in European Mine Waters: Sulphides, Evaporites or Seawater? *Int. J. Coal Geol.* 232, 103619. doi:10.1016/j.coal.2020.103619

Banks, D., Steven, J., Black, A., and Naismith, J. (2022). Conceptual Modelling of Two Large-Scale Mine Water Geothermal Energy Schemes: Felling, Gateshead, UK. *Int. J. Environ. Res. Public Health* 19 (3), 1643. doi:10.3390/ijerph19031643

Banks, S. B. (2003). The UK Coal Authority Minewater Treatment Scheme Programme. *Water Environ. J.* 17 (2), 117–122. doi:10.1111/j.1747-6593.2003.tb00444.x

Banks, D. (2021). "Fessing up: Risks and Obstacles to Mine Water Geothermal Energy," in Proceedings Mine Water Heating and Cooling; A 21st Century Resource for Decarbonisation, March 10-11, 2021 (British Geological Survey, UK Department for Business, Energy and Industrial Strategy and IEA Geothermal).

Bluck, B. J. (1984). Pre-Carboniferous History of the Midland Valley of Scotland. *Trans. R. Soc. Edinb. Earth Sci.* 75 (2), 275–295. doi:10.1017/S0263593300013900

BoilerGuide (2022). *What Size Heat Pump Do I Need?* Available at: www.boilerguide.co.uk/articles/size-heat-pump-need (Accessed 03 03, 2022).

British Geological Survey (2008). *Ayr. Scotland Sheet 14W and Part of 13. Bedrock. 1:50 000 Geology Series*. Nottingham, United Kingdom: British Geological Survey.

British Standards Institution (2009). *BS EN ISO 10304-1: Water Quality. Determination of Dissolved Anions by Liquid Chromatography of Ions. Determination of Bromide, Chloride, Fluoride, Nitrate, Nitrite, Phosphate and Sulphate*. London, United Kingdom: British Standards Institution. 978 0 580 65935 5.

British Standards Institution (2018). *PD CEN/TS 17197:2018 Construction Products: Assessment of Release of Dangerous Substances - Analysis of Inorganic Substances in Digests and Eluates - Analysis by Inductively Coupled Plasma - Optical Emission Spectrometry (ICP-OES) Method*. 9780580850585.

Brown, M. M. E., Jones, A. L., Leighfield, K. G., and Cox, S. J. (2002). Fingerprinting Mine Water in the Eastern Sector of the South Wales Coalfield: Mine Water Hydrogeology and Geochemistry. *Geol. Soc. Lond. Spec. Publ.* 198, 275–286. doi:10.1144/GSL.SP.2002.198.01.18

Bullock, L. A., Parnell, J., Perez, M., Boyce, A., Feldmann, J., and Armstrong, J. G. T. (2018). Multi-stage Pyrite Genesis and Epigenetic Selenium Enrichment of Greenburn Coals (East Ayrshire). *Scott. J. Geol.* 54 (1), 37–49. doi:10.1144/sjg2017-010

Burnside, N. M., Banks, D., and Boyce, A. J. (2016a). Sustainability of Thermal Energy Production at the Flooded Mine Workings of the Former Caphouse Colliery, Yorkshire, United Kingdom. *Int. J. Coal Geol.* 164, 85–91. doi:10.1016/j.coal.2016.03.006

Burnside, N. M., Banks, D., Boyce, A. J., and Athresh, A. (2016b). Hydrochemistry and Stable Isotopes as Tools for Understanding the Sustainability of Minewater Geothermal Energy Production from a 'standing Column' Heat Pump System: Markham Colliery, Bolsover, Derbyshire, UK. *Int. J. Coal Geol.* 165, 223–230. doi:10.1016/j.coal.2016.08.021

Cameron, I. B., and Stephenson, D. (1985). "British Regional Geology: The Midland Valley of Scotland London," in *British Geological Survey & NERC*. 3rd ed (London, United Kingdom: H.M.S.O), 172.

Carmody, R. W., Plummer, N., Busenberg, E., and Coplen, T. B. (1998). *Methods for Collection of Dissolved Sulfate and Sulfide and Analysis of Their Sulfur Isotopic Composition*. Reston, VA: U.S. Geological Survey, 97–234.

Chen, X., Zheng, L., Dong, X., Jiang, C., and Wei, X. (2020). Sources and Mixing of Sulfate Contamination in the Water Environment of a Typical Coal Mining City, China: Evidence from Stable Isotope Characteristics. *Environ. Geochem. Health* 42 (9), 2865–2879. doi:10.1007/s10653-020-00525-2

Coleman, M. L., and Moore, M. P. (1978). Direct Reduction of Sulphates to Sulphur Dioxide for Isotopic Analysis. *Anal. Chem.* 28, 199–260.

Committee on Climate Change (2019). *UK Housing: Fit for the Future?* London: Committee on Climate Change, 135.

Crooks, J. (2018). "Clean Energy from the Coalfields," in Proceedings Mining the Future: Innovation in heating and cooling, The Hague, The Netherlands, October 3rd 2018.

Davis, S. N., Whittemore, D. O., and Fabryka-Martin, J. (1998). Uses of Chloride/Bromide Ratios in Studies of Potable Water. *Ground Water* 36 (2), 338–350. doi:10.1111/j.1745-6584.1998.tb01099.x

Dean, G., Craig, J., Gerali, F., MacAulay, F., and Sorkhabi, R. (2018). "The Scottish Oil-Shale Industry from the Viewpoint of the Modern-Day Shale-Gas Industry," in *History of the European Oil and Gas Industry* (Geological Society of London).

Donnelly, T., Waldron, S., Tait, A., Dougans, J., and Bearhop, S. (2001). Hydrogen Isotope Analysis of Natural Abundance and Deuterium-Enriched Waters by Reduction over Chromium On-Line to a Dynamic Dual Inlet Isotope-Ratio Mass Spectrometer. *Rapid Commun. Mass Spectrom.* 15 (15), 1297–1303. doi:10.1002/rcm.361

Energy Saving Trust (2021). *Renewable Heat in Scotland 2020 Report*. Edinburgh: Energy Savings Trust for the Scottish Government, 38.

SUPPLEMENTARY MATERIAL

The Supplementary Material for this article can be found online at: https://www.escubed.org/articles/10.3389/esss.2022.10056/full#supplementary-material

Available at: https://energysavingtrust.org.uk/wp-content/uploads/2021/10/Renewable-heat-in-Scotland-2020-report-version-2.pdf.

Environmental Agency (2021). *Mine Waters: Challenges for the Water Environment*. Bristol: Environmental Agency, 22. Available at: https://www.gov.uk/government/publications/mine-waters-challenges-for-the-water-environment.

Farr, G., Sadasivam, S., ManjuWatson, I. A., Thomas, H. R., and Tucker, D. (2016). Low Enthalpy Heat Recovery Potential from Coal Mine Discharges in the South Wales Coalfield. *Int. J. Coal Geol.* 164, 92–103. doi:10.1016/j.coal.2016.05.008

Farr, G., Busby, J., Wyatt, L., Crooks, J., Schofield, D. I., and Holden, A. (2021). The Temperature of Britain's Coalfields. *Q. J. Eng. Geol. Hydrogeo.* 54 (3), qjegh2020–2109. doi:10.1144/qjegh2020-109

Fichtner, V., Strauss, H., Immenhauser, A., Buhl, D., Neuser, R. D., and Niedermayr, A. (2017). Diagenesis of Carbonate Associated Sulfate. *Chem. Geol.* 463, 61–75. doi:10.1016/j.chemgeo.2017.05.008

Gillespie, M. R., Crane, E. J., and Barron, H. F. (2013). *Study into the Potential for Deep Geothermal Energy in Scotland*. British Geological Survey Commissioned Report, Nottingham, United Kingdom, CR/12/131, 129

Gzyl, G., and Banks, D. (2007). Verification of the "First Flush" Phenomenon in Mine Water from Coal Mines in the Upper Silesian Coal Basin, Poland. *J. Contam. Hydrol.* 92 (1), 66–86. doi:10.1016/j.jconhyd.2006.12.001

Hall, J., Glendinning, S., and Younger, P. (2005). "Is Mine Water a Source of Hazardous Gas?," in Proceedings of the 9th International Mine Water Association Congress 2005, Oviedo, Spain, September 5–7, 2005.

Harker, S. D., and Trewin, N. H. (2002). "Cretaceous," in *The Geology of Scotland* (Geological Society of London).

Haunch, S. M., A., and McDermott, C. (2021). "Variability in Mine Waste Mineralogy and Water Environment Risks: a Case Study on the River Almond Catchment, Scotland," in IMWA 2021 - Mine Water Management for Future Generations. Editors P. Stanley, C. Wolkersdorfer, and K. Wolkersdorfer (International Mine Water Association). Available at: https://www.imwa.info/docs/imwa_2021/IMWA2021_Haunch_181.pdf.

James Hutton Institute (2016). *Feasibility Report of Fortissat Community Minewater Geothermal Energy District Heating Network*, 104. Edinburgh: The Scottish Government, 978.

Janson, E., Boyce, A. J., Burnside, N., and Gzyl, G. (2016). Preliminary Investigation on Temperature, Chemistry and Isotopes of Mine Water Pumped in Bytom Geological Basin (USCB Poland) as a Potential Geothermal Energy Source. *Int. J. Coal Geol.* 164, 104–114. doi:10.1016/j.coal.2016.06.007

Jessop, A. M., MacDonald, J. K., and Spence, H. (1995). Clean Energy from Abandoned Mines at Springhill, Nova Scotia. *Energy Sources.* 17 (1), 93–106. doi:10.1080/00908319508946072

Jones, N. S. (2007). *The West Lothian Oil-Shale Formation: Results of a Sedimentological Study*. Internal Report IR/05/046. Nottingham, United Kingdom: British Geological Survey, 63.

Kampschulte, A., and Strauss, H. (2004). The Sulfur Isotopic Evolution of Phanerozoic Seawater Based on the Analysis of Structurally Substituted Sulfate in Carbonates. *Chem. Geol.* 204 (3), 255–286. doi:10.1016/j.chemgeo.2003.11.013

Kampschulte, A., Bruckschen, P., and Strauss, H. (2001). The Sulphur Isotopic Composition of Trace Sulphates in Carboniferous Brachiopods: Implications for Coeval Seawater, Correlation with Other Geochemical Cycles and Isotope Stratigraphy. *Chem. Geol.* 175 (1), 149–173. doi:10.1016/S0009-2541(00)00367-3

Lenntech (2022). *Composition of Seawater*. Available at: https://www.lenntech.com/composition-seawater.htm (Accessed 03 03, 2022).

Limberger, J., Boxem, T., Pluymaekers, M., Bruhn, D., Manzella, A., Calcagno, P., et al. (2018). Geothermal Energy in Deep Aquifers: A Global Assessment of the Resource Base for Direct Heat Utilization. *Renew. Sustain. Energy Rev.* 82, 961–975. doi:10.1016/j.rser.2017.09.084

Loredo, C., Ordonez, A., Garcia-Ordiales, E., Alvarez, R., Roqueni, N., Cienfuegos, P., et al. (2017). Hydrochemical Characterization of a Mine Water Geothermal Energy Resource in NW Spain. *Sci. Total Environ.* 576, 59–69. doi:10.1016/j.scitotenv.2016.10.084

Mayes, W. M., Perks, M. T., Large, A. R. G., Davis, J. E., Gandy, C. J., Orme, P. A. H., et al. (2021). Effect of an Extreme Flood Event on Solute Transport and Resilience of a Mine Water Treatment System in a Mineralised Catchment. *Sci. Total Environ.* 750, 141693. doi:10.1016/j.scitotenv.2020.141693

Millward, D., Davies, S. J., Williamson, F., Curtis, R., Kearsey, T. I., Bennett, C. E., et al. (2018). Early Mississippian Evaporites of Coastal Tropical Wetlands. *Sedimentology* 65 (7), 2278–2311. doi:10.1111/sed.12465

Monaghan, A. A., O Dochartaigh, B., Fordyce, F., Loveless, S., Entwisle, D., Quinn, M., et al. (2017). *UKGEOS - Glasgow Geothermal Energy Research Field Site (GGERFS): Initial Summary of the Geological Platform*. OR/17/006, Nottingham, UK: British Geological Survey, 205.

Monaghan, A. A., Damaschke, M., Starcher, V., Fellgett, M. W., Kingdon, A., Kearsey, T., et al. (2021). *UKGEOS Glasgow GGC01 Final Borehole Information Pack: NERC EDS*. Nottingham, United Kingdom: National Geoscience Data Centre.

Monaghan, A. A., Bateson, L., Boyce, A. J., Burnside, N. M., Chambers, R., de Rezende, J. R., et al. (2022a). Time Zero for Net Zero: A Coal Mine Baseline for Decarbonising Heat: Earth Science. *Syst. Soc.* 2, 10054. doi:10.3389/esss.2022.10054

Monaghan, A. A., Starcher, V., Barron, H. F., Shorter, K., Walker-Verkuil, K., Elsome, J., et al. (2022b). Drilling into Mines for Heat: Geological Synthesis of the UK Geoenergy Observatory in Glasgow and Implications for Mine Water Heat Resources. *Q. J. Eng. Geol. Hydrogeo.* 55 (1), qjegh2021–2033. doi:10.1144/qjegh2021-033

Monaghan, A. A. (2014). *The Carboniferous Shales of the Midland Valley of Scotland: Geology and Resource Estimation*. London, UK: British Geological Survey for Department of Energy and Climate Change.

Nelson, S. T. (2000). A Simple, Practical Methodology for Routine VSMOW/SLAP Normalization of Water Samples Analyzed by Continuous Flow Methods. *Rapid Commun. Mass Spectrom.* 14 (12), 1044–1046. doi:10.1002/1097-0231(20000630)14:12<1044:aid-rcm987>3.0.co;2-3

Nuttall, C. A., and Younger, P. L. (2004). Hydrochemical Stratification in Flooded Underground Mines: An Overlooked Pitfall. *J. Contam. Hydrol.* 69 (1-2), 101–114. doi:10.1016/S0169-7722(03)00152-9

O Dochartaigh, B. E., Smedley, P. L., MacDonald, A. M., Darling, W. G., and Homoncik, S. (2011). *Baseline Scotland : Groundwater Chemistry of the Carboniferous Sedimentary Aquifers of the Midland Valley*. Open Report, OR/11/021. Nottingham, United Kingdom: British Geological Survey, 105.

Ó Dochartaigh, B. É., MacDonald, A. M., Fitzsimons, V., and Ward, R. (2015). *Scotland's Aquifers and Groundwater Bodies*. Survey Open Report, OR/15/028. Nottingham, United Kingdom: British Geological, 76.

Oglethorpe, M. K. (2006). *Scottish Collieries: An Inventory of the Scottish Coal Industry in the Nationalized Era*. Edinburgh: Royal Commission on the Ancient and Historical Monuments of Scotland. 978-1-902419-47-3.

Peiffer, S., and Wan, M. (2016). "Reductive Dissolution and Reactivity of Ferric (Hydr)oxides: New Insights and Implications for Environmental Redox Processes," in *Iron Oxides*, 31–52.

Present, T. M., Adkins, J. F., and Fischer, W. W. (2020). Variability in Sulfur Isotope Records of Phanerozoic Seawater Sulfate. *Geophys. Res. Lett.* 47–18. doi:10.1029/2020GL088766

Ramos, E. P., Breede, K., and Falcone, G. (2015). Geothermal Heat Recovery from Abandoned Mines: a Systematic Review of Projects Implemented Worldwide and a Methodology for Screening New Projects. *Environ. Earth Sci.* 73 (11), 6783–6795. doi:10.1007/s12665-015-4285-y

Rawson, P. F. (2006). "Cretaceous: Sea Levels Peak as the North Atlantic Opens," in *The Geology of England and Wales*. Editors P. J. Brenchley, and P. F. Rawson (Geological Society of London).

Reimann, C., Filzmoser, P., Garrett, R., and Dutter, R. (2008). *Statistical Data Analysis Explained*, 359. Chichester, England: John Wiley & Sons.

Reinecker, J., Gutmanis, J., Foxford, A., Cotton, L., Dalby, C., and Law, R. (2021). *Geothermal Exploration and Reservoir Modelling of the United*

Downs Deep Geothermal Project. Cornwall (UK): Geothermics, 97. doi:10.1016/j.geothermics.2021.102226
Rippon, J., Read, W. A., and Park, R. G. (1996). The Ochil Fault and the Kincardine Basin: Key Structures in the Tectonic Evolution of the Midland Valley of Scotland. *J. Geol. Soc. Lond.* 153 (4), 573–587. doi:10.1144/gsjgs.153.4.0573
Rowley, A. (2013). *Questions Raised over Mining Operations in Fife*. Available at: http://www.alexrowley.org/questions-raised-over-mining-operations-in-fife/(Accessed 05 14, 2021).
Scottish Government (2020). *Update to the Climate Change Plan 2018 – 2032: Securing a Green Recovery on a Path to Net Zero*. Edinburgh, United Kingdom: Scottish Government. 255. 9781800044302
Scottish Government (2022). *New Build Heat Standard Consultation: Part II*. 35. 9781804356463
Smith, J., and Colls, J. J. (1996). Groundwater Rebound in the Leicestershire Coalfield: Water and. *Water Environ. J.* 10 (4), 280–289. doi:10.1111/j.1747-6593.1996.tb00046.x
Spears, D. A., and Amin, M. A. (1981). Geochemistry and Mineralogy of Marine and Non-marine Namurian Black Shales from the Tansley Borehole, Derbyshire. *Sedimentology* 28 (3), 407–417. doi:10.1111/j.1365-3091.1981.tb01689.x
Steven, J. (2021). "From Venture Pit to Walker Shore, Coal and Heat and Fathoms of Core': Mine Water Heat Exploitation in Newcastle/Gateshead," in Proceedings 2021 Mine Water Geothermal Energy Symposium, 10th-11th March 2021 (Webinar).
Stumm, W., and Sulzberger, B. (1992). The Cycling of Iron in Natural Environments: Considerations Based on Laboratory Studies of Heterogeneous Redox Processes. *Geochim. Cosmochim. Acta* 56 (8), 3233–3257. doi:10.1016/0016-7037(92)90301-X
The Coal Authority (2021). *Annual Report and Accounts 2020-21*. Mansfield, United Kingdom: The Coal Authority, 115. 978-1-5286-2770-2.
The Coal Authority (2022). *Interactive Map*. Available at: https://mapapps2.bgs.ac.uk/coalauthority/home.html (Accessed 11 25, 2021).
Thomson, M. E. (1978). *IGS Studies of the Geology of the Firth of Forth and its Approaches*, 70. London: HMSO. 0118840657.
Tostevin, R., Turchyn, A. V., Farquhar, J., Johnston, D. T., Eldridge, D. L., Bishop, J. K. B., et al. (2014). Multiple Sulfur Isotope Constraints on the Modern Sulfur Cycle. *Earth Planet. Sci. Lett.* 396, 14–21. doi:10.1016/j.epsl.2014.03.057
Trueman, A. (1954). *The Coalfields of Great Britain*. London: Edward Arnold, 396. doi:10.1017/S0016756800653530016-7568
Tukey, J. W. (1977). *Exploratory Data Analysis*. Biometrical Journal, 4. London, Amsterdam, Don Mills, Ontario: Sydney Addison-Wesley Publishing Company. Reading, Mass. — Menlo Park, Cal. doi:10.1002/bimj.47102304080323-3847
UK Government (2021a). *Heat and Buildings Strategy*. London, United Kingdom: The UK Government Open Government Licence, 244. 978-1-5286-2459-6
UK Government (2021b). *Net Zero Strategy*: Build Back Greener. 368. 978-1-5286-2938-6. Available at: https://assets.publishing.service.gov.uk/government/uploads/system/uploads/attachment_data/file/1033990/net-zero-strategy-beis.pdf.
Underhill, J. R., Monaghan, A. A., and Browne, M. A. E. (2008). Controls on Structural Styles, Basin Development and Petroleum Prospectivity in the Midland Valley of Scotland. *Mar. Petroleum Geol.* 25 (10), 1000–1022. doi:10.1016/j.marpetgeo.2007.12.002
United Nations (2019). "Report of the Secretary-General on the 2019 Climate Action Summit and the Way Forward in 2020," in Proceedings Climate Action Summit, New York City, 11th December 2019, 38.
Verhoeven, R., Willems, E., Harcouët-Menou, V., De Boever, E., Hiddes, L., Veld, P. O. t., et al. (2014). Minewater 2.0 Project in Heerlen the Netherlands: Transformation of a Geothermal Mine Water Pilot Project into a Full Scale Hybrid Sustainable Energy Infrastructure for Heating and Cooling. *Energy Procedia* 46, 58–67. doi:10.1016/j.egypro.2014.01.158
Wallis, G. (2017). Restoring the Elsecar Newcomen Engine—High Ideals, Deep Mysteries. *Int. J. Hist. Eng. Technol.* 87 (2), 154–164. doi:10.1080/17581206.2018.1462629
Walls, D. B., Banks, D., Boyce, A. J., and Burnside, N. M. (2021). A Review of the Performance of Minewater Heating and Cooling Systems. *Energies* 14 (19), 6215. doi:10.3390/en14196215
Waters, C. N., Browne, M. A. E., Dean, M. T., and Powell, J. H. (2007). *Lithostratigraphical Framework for Carboniferous Successions of Great Britain (Onshore)*. Research Report, RR/10/07. Nottingham, United Kingdom: British Geological Survey, 174.
Watson, I. A. (2007). "Managing Minewater in Abandoned Coalfields Using Engineered Gravity Discharges," in IMWA Symposium 2007: Water in Mining Environments, Cagliari, Italy, May 27–31, 2007. Editors R. Cidu, and F. Frau.
Whitworth, K., England, A., and Parry, D. (2012). *Long-term Changes in the Quality of Polluted Minewater Discharges from Abandoned Underground Coal Workings in Scotland*. Nottinghamshire, United Kingdom.
Wood, S. C., Younger, P. L., and Robins, N. S. (1999). Long-term changes in the quality of polluted minewater discharges from abandoned underground coal workings in Scotland. *Q. J. Eng. Geol. Hydro.* 32 (1), 69–79. doi:10.1144/gsl.Qjeg.1999.032.P1.05
Wu, N., Farquhar, J., and Strauss, H. (2014). δ34S and Δ33S Records of Paleozoic Seawater Sulfate Based on the Analysis of Carbonate Associated Sulfate. *Earth Planet. Sci. Lett.* 399, 44–51. doi:10.1016/j.epsl.2014.05.004
Younger, P. L., and Adams, R. (1999). *Predicting Mine Water Rebound R&D Technical Report W179*. Bristol, United Kingdom: Environment Agency.
Younger, P. L., and LaPierre, A. B. (2000). Uisge Mèinne': Mine Water Hydrogeology in the Celtic Lands, from *Kernow* (Cornwall, UK) to *Ceap Breattain* (Cape Breton, Canada). *Geol. Soc. Lond. Spec. Publ.* 182 (1), 35–52. doi:10.1144/GSL.SP.2000.182.01.04
Younger, P., and Robins, N. (2002). Challenges in the Characterization and Prediction of the Hydrogeology and Geochemistry of Mined Ground. *Geol. Soc. Lond. Spec. Publ.* 198, 1–16. doi:10.1144/GSL.SP.2002.198.01.01
Younger, P. L., Boyce, A. J., and Waring, A. J. (2015). Chloride Waters of Great Britain Revisited: from Subsea Formation Waters to Onshore Geothermal Fluids. *Proc. Geologists'. Assoc.* 126 (4-5), 453–465. doi:10.1016/j.pgeola.2015.04.001
Younger, P. L. (1997). The Longevity of Minewater Pollution: A Basis for Decision-Making. *Sci. Total Environ.* 194-195, 457–466. doi:10.1016/S0048-9697(96)05383-1
Younger, P. L. (2000a). "Iron," in *Diffuse Pollution Impacts*. Editors B. J. D. Darcy, J. B. Ellis, R. C. Ferrier, A. Jenkins, and R. Dils (Terence Dalton Publishers, Lavenham, for Chartered Institution of Water and Environmental Management), 95–104.
Younger, P. L. (2000b). Predicting Temporal Changes in Total Iron Concentrations in Groundwaters Flowing from Abandoned Deep Mines: a First Approximation. *J. Contam. Hydrology* 44 (1), 47–69. doi:10.1016/S0169-7722(00)00090-5
Younger, P. L. (2001). Mine Water Pollution in Scotland: Nature, Extent and Preventative Strategies. *Sci. Total Environ.* 265 (1), 309–326. doi:10.1016/S0048-9697(00)00673-2
Younger, P. L. (2007). *Groundwater in the Environment: An Introduction*, 318. UK & Malden, Massachusetts: Oxford.